Exploring the Surface of Aqueous Solutions

X-ray photoelectron spectroscopy studies using a liquid micro-jet

Josephina Werner
Faculty of Natural Resources and Agricultural Sciences
Department of Chemistry and Biotechnology
Uppsala

Doctoral Thesis
Swedish University of Agricultural Sciences
Uppsala 2015

Acta Universitatis agriculturae Sueciae

2015:133

ISSN 1652-6880
ISBN (print version) 978-91-576-8464-6
ISBN (electronic version) 978-91-576-8465-3

Acta Universitatis Upsaliensis
Uppsala

2015

Digital comprehensive summaries of Uppsala dissertations from the Faculty of Science and Technology 1313
ISSN 1651-6214
ISBN 978-91-554-9399-8
urn:nbn:se:uu:diva-265210

Print: SLU Service/Repro, Uppsala 2015

Exploring the Surface of Aqueous Solutions. X-ray photoelectron spectroscopy studies on a liquid micro-jet.

Abstract

The surface behavior of biologically or atmospherically relevant chemical compounds in aqueous solution has been studied using surface-sensitive X-ray photoelectron spectroscopy (XPS). The aim is to provide information on the molecular-scale composition and distribution of solutes in the surface region of aqueous solutions. In the first part, the distribution of solutes in the surface region is discussed, where in particular single molecular species are studied. Concentration-dependent studies on succinic acid and various alkyl-alcohols, where also parameters such as pH and branching are varied, are analyzed using different approaches that allow the quantification of surface concentrations. Furthermore, due to the sensitivity of XPS to the chemical state, reorientation of linear and branched alkyl-alcohols at the aqueous surface as a function of concentration is observed. The results are further discussed in terms of hydrophilic and hydrophobic interactions in the interfacial region, where the three-dimensional hydrogen bonded water structure terminates. In the second part, mixed solutions of compounds, both ionic and molecular, are inspected. Again concentration, but also co-dissolution of other chemical compounds, are varied and differences in the spatial distribution and composition of the surface region are discussed. It is found that the guanidinium ion has an increased propensity to reside at the surface, which is explained by strong hydration in only two dimensions and only weak interactions between the aromatic π-system and water. Ammonium ions, on the other hand, which require hydration in three dimensions, are depleted from the surface region. The presence of strongly hydrated electrolytes out-competes neutral molecules for hydrating water molecules leading to an enhanced abundance of molecules, such as succinic acid, in the interfacial region. The partitioning is quantified and discussed in the context of atmospheric science, where the impact of the presented results on organic loading of aerosol particles is emphasized.

Keywords: X-ray Photoelectron spectroscopy, liquid micro-jet, air-water interface, inorganic salt, carboxylic acid, alcohol, isomers, hydration.

Josephina Werner, Department of Physics and Astronomy, Box 516, Uppsala University, SE- 751 20 Uppsala, Sweden. Department of Chemistry and Biotechnology, Box 7015, Swedish University of Agricultural Sciences, SE-750 07 Uppsala, Sweden.

UPPSALA
UNIVERSITET

This doctoral thesis presents research carried out at Uppsala University, Department of Physics and Astronomy, and the Swedish University of Agricultural Sciences, Department of Chemistry and Biotechnology. It is published at both institutions.

Acta Universitatis Upsaliensis
Uppsala
2015

Digital comprehensive summaries of Uppsala dissertations from the Faculty of Science and Technology 1313
ISSN 1651-6214
ISBN 978-91-554-9399-8
urn:nbn:se:uu:diva-265210

Acta Universitatis agriculturae Sueciae
2015:133

ISSN 1652-6880
ISBN (print version) 978-91-576-8464-6
ISBN (electronic version) 978-91-576-8465-3

To my family

List of papers

This thesis is based on the following papers, which are referred to in the text by their Roman numerals.

I. **Succinic Acid in Aqueous Solutions: Connecting Microscopic Surface Composition and Macroscopic Surface Tension**
Josephina Werner, Jan Julin, Maryam Dalirian, Nønne L. Prisle, Gunnar Öhrwall, Ingmar Persson, Olle Björneholm and Ilona Riipinen
Physical Chemistry Chemical Physics, **16**: 21486-21495 (2014)

II. **Surface Behavior of Amphiphiles in Aqueous Solution: A Comparison Between Different Pentanol Isomers**
Marie-Madeleine Walz, Carl Caleman, Josephina Werner, Victor Ekholm, Daniel Lundberg, Nønne L. Prisle, Gunnar Öhrwall and Olle Björneholm
Physical Chemistry Chemical Physics, **17**: 14036-14044 (2015)

III. **Alcohols at the Aqueous Surface: Chain Length and Isomer Effects**
Marie-Madeleine Walz, Josephina Werner, Victor Ekholm, Nønne L. Prisle, Gunnar Öhrwall and Olle Björneholm
Submitted

IV. **Surface Behavior of Aqueous Guanidinium and Ammonium ions: A Comparative Study by Photoelectron Spectroscopy and Molecular Dynamics**
Josephina Werner, Erik Wernersson, Victor Ekholm, Niklas Ottosson, Gunnar Öhrwall, Jan Heyda, Ingmar Persson, Johan Söderström, Pavel Jungwirth and Olle Björneholm
Journal of Physical Chemistry B, **118**: 7119-7127 (2014)

V. **Surface Enhancement of Organic Acids by Inorganic Salts with Implications for Atmospheric Nanoparticles**
Josephina Werner, Maryam Dalirian, Marie-Madeleine Walz, Victor Ekholm, Ulla Wideqvist, Sam J. Lowe, Gunnar Öhrwall, Ingmar Persson, Ilona Riipinen and Olle Björneholm
In manuscript

Extended bibliography

The following publications are not covered in this thesis.

1. **Deeper Insight into Depth-Profiling of Aqueous Solutions Using Photoelectron Spectroscopy**
   Olle Björneholm, Josephina Werner, Niklas Ottosson, Gunnar Öhrwall, Victor Ekholm, Bernd Winter, Isaak Unger, Johan Söderström
   Journal of Physical Chemistry C, **118**: 29333-29339 (2014)

2. **Acid-Base Speciation of Carboxylate Ions in the Surface Region of Aqueous Solutions in the Presence of Ammonium and Aminium Ions**
   Gunnar Öhrwall, Nønne L. Prisle, Niklas Ottosson, Josephina Werner, Victor Ekholm, Marie-Madeleine Walz and Olle Björneholm
   Journal of Physical Chemistry B, **119**: 4033-4040 (2015)

Comments on my personal contribution

The work presented in this thesis is the results of joint efforts, where many people were/are involved at different stages of the experimental and theoretical work. I have actively taken part in conducting experiments for all projects that are presented and my relative contribution is reflected in my position in the author list of each paper. For papers **I**, **IV**, and **V**, I was main responsible throughout the project, including planning and performance of the experimental work, analysis of obtained data and writing of the article. In papers **II** and **III** I have contributed with experimental work and was involved in different stages of the analysis and discussion of the results. I was working close with collaborators that perform molecular dynamics simulations, physico-chemical modeling and supplementary experiments. I joined discussions on results and planned further contributions, complementing the results from X-ray photoelectron spectroscopy experiments to illustrate the implications of the obtained results on atmospheric science and surface phenomena in general.

Contents

1. Introduction and background

Water covers most of the Earth's surface and is the fundamental precondition for life. It shapes mountains and coastlines, exists as rain, hail or clouds and plays a crucial role as mediator of biological important chemical reactions. The universal solvent is a molecule that is made up from one oxygen and two hydrogen atoms, which possesses a few extraordinary anomalies that distinguishes this liquid from others. Water expands when frozen, but it is more dense at low temperature than in its solid form, which is the reason why ice floats on the surface of e.g. lakes. The microscopic origin of many of its macroscopic properties is still not fully explained and todays' scientists try to conceive a detailed picture of the roles and properties of water.

Water is abundant in many forms and aspects of life, but it is rarely found in its pure form. Typically it appears as aqueous solutions in our environment, as in oceans, in soil or in living organisms. In such, it occupies small spaces together with e.g. electrolytes and proteins, as it is the case in biological cells. Here, water controls the folding patterns of proteins and steers the transport through cell membranes. In the atmosphere, water exists as vapor and in small aerosol droplets, which have a high surface-to-volume ratio. This means that the surface is important especially for these small systems and changes in the particles' surface can lead to substantial variations of their properties. Water in the surface region serves as mediator of transitions between the gaseous and the liquid phase. Hence, interfacial water of environmental systems yields essential features for transition and cycle processes.

Many of waters' unique properties stem from the ability to form hydrogen bonds. The attractive forces between water molecules lead to a network with water molecules bound to one another in three dimensions. At the surface, this hydrogen bonding network is terminated and the residing molecules have a reduced amount of hydrogen bonding partners available compared with solutes in the bulk of the liquid. This results in various surface-specific phenomena, for pure water but also for aqueous solutions. Such effects are investigated both theoretically and experimentally, to shed light on interfacial properties of solutes and solvents, which are distinct from that of bulk solutions [1, 2]. A key question in this field is the composition of the surface in comparison with the bulk of a solution. For example, the preference of some ionic species to reside close to the aqueous surface [3, 4], which were long believed to be strongly depleted, yields a different compound distribution in the interfacial region as compared with the homogeneously distributed compounds in the bulk of a solution. The hydrophobicity of the water-vapor interface enables

a strong stabilization of amphiphilic molecules that can cover the surface to different degrees. The enrichment or depletion of the waters' own ions, hydronium and hydroxide, from the aqueous surface and possible consequences for acid-base chemistry in the surface are investigated and contrary results are reported, see e.g. references 5–7.

In general, factors that determine a compounds' surface propensity, which is a measure of the universal or compound-specific tendency of a species to reside close to the air-water interface, and degree of enrichment/depletion need to be further examined and quantified to fully understand the governing parameters leading to the observed behaviors. Furthermore, a less explored area of this research field concerns inter-solute interactions, e.g. between different inorganic ions or between organic molecules and ions, and the effect of the aqueous surface in this context. Such interactions may alter the interfacial distribution of solute species strongly.

For small atmospheric droplets with high surface-to-volume ratio, an alteration of structure and composition of the surface may lead to substantial changes of the particles' properties. For example, the ability of the droplets to transport species between the surrounding gas and the inside of the particles or more macroscopic properties like light reflection and absorption, can be affected. The detailed understanding of light-matter interactions on the molecular scale, may lead to insights concerning the sunlight reflection of clouds, which are connected to the present uncertainty of warming and cooling effects of clouds on the climate [8]. General trends of these effects are known, but global climate models need detailed and especially quantified inputs to refine and reduce uncertainties of climate prognoses.

A variety of experimental techniques including spectroscopic methods are used to probe the microscopic structure and dynamics of the bulk of aqueous solutions, e.g., nuclear magnetic resonance (NMR) spectroscopy, dielectric relaxation, pump-probe spectroscopy and scattering techniques, such as large angle X-ray scattering, X-ray and neutron diffraction. But also theoretical approaches, such as molecular dynamics (MD) simulations or density functional theory calculations, are commonly used for similar purposes. Only a few experimental tools are available for probing the surface of aqueous solutions directly. Sum frequency generation spectroscopy, second harmonic generation spectroscopy, grazing incidence X-ray diffraction and X-ray photoelectron spectroscopy (XPS) are such experimental tools. In particular, XPS is applied to e.g. thin liquid jets or deliquescent salt crystals. The technique itself, which mainly reveals changes in the electronic structure and spatial distribution of bulk or interfacial matter, is well established and has been successfully applied for the characterization of solids, gases, clusters. Liquid samples have represented a major challenge for a long time, as the experiment requires the sample to be in an evacuated chamber and the volatility of liquid samples results in too high background pressures. Technical advances, namely by K. Siegbahn and co-workers in the 70's [9] and M. Faubel and co-workers in

80's [10], finally enable the use of XPS in its full power also on rather volatile liquid samples. Since then the electronic structure and chemical composition of various mixtures and also pure liquids have been explored using this technique.

In this thesis, XPS was applied to aqueous solutions with ionic and molecular solutes to garner information on the hydration and composition of the surface region of aqueous solutions. The presented projects are mainly motivated by environmental and atmospheric sciences. Samples were chosen that represent typical model systems, which are similar to real environmental solutions, such as the ocean or cloud droplets. In particular compounds that are believed to play an important role in aerosol activation and growth processes, such as low-volatile organic compounds, are studied [11]. Also mixed solutions that are important in biochemistry have been investigated. Often the study of complex compounds, such as proteins or DNA, is too difficult to study immediately. The investigation of important functional groups, such as guanidinium and ammonium ions, provide valuable information that enable the understanding of future results on more complex mixtures.

2. Chemistry and thermodynamics of aqueous solutions

As a major part of the thesis deals with solutions of inorganic and organic compounds, fundamental principles of these systems are provided in this chapter. Furthermore, a few important concepts of interfacial phenomena and general principles used in atmospheric science are introduced.

2.1 Water as a chemical

Water is an odorless clear liquid at room temperature, that serves as solvent for many substances. It is a molecule composed of two hydrogen atoms covalently bound to one oxygen atom. In the gaseous phase the angle between the two hydrogen atoms is 104.5°. A dipole stretches over the molecule along the plane of reflection symmetry, which is created mostly by the strong electronegativity of the oxygen atom. In its ground state, the electronic configuration of a water molecule is the following:

$$(1a_1)^2\ (2a_1)^2\ (1b_2)^2\ (3a_1)^2\ (1b_1)^2.$$

The inner-most molecular orbital $1a_1$ is an only slightly perturbed O1s atomic orbital. The molecular orbitals $2a_1$ and $3a_1$ are partly involved in bondings, while the $1b_2$ is strictly utilized in bonds and the $1b_1$ is not involved in bonds [12]. The latter is easily available from photoemission (PE) spectra at low binding energies, i.e. 12.62 eV for gaseous water or 11.16 eV for liquid water [13, 14].

As this thesis solely deals with liquid water, its diverse properties in other aggregation states will be omitted here. In gases the interactions between molecules are much weaker than their thermal energy. In solid matter, on the other hand, the interactions are so strong that species are strongly confined, often into a rigid structure, which reduces the motion of the species to a minimum. Liquids can be viewed as an intermediate between the two aggregation states, as the interactions between the species are usually on the order of their thermal energy. The density is often very similar to the one of solids, but the dynamics are more similar to the ones of gases.

Water has the famous property of being able to form a strong hydrogen bonding network. In pure water this consists on average of four water molecules

around one water molecule, which are arranged in a tetrahedral-like conformation [15].

Before focusing on properties of aqueous solutions, autoionization of pure water and properties of the hydronium (H_3O^+) and hydroxide (OH^-) ions are briefly mentioned. By changing the pH of pure liquid water, water molecules create hydronium and hydroxide ions. This process is called self-ionization or autoionization of water, see equation 2.1.

$$2\,H_2O \rightleftharpoons H_3O^+ + OH^- \tag{2.1}$$

At room temperature the reaction constant K_w, which is in that case called the ionic product of water, is given as $K_w = c_{H_3O^+} \cdot c_{OH^-} = 10^{-14}$ $(mol/dm^3)^2$, where $c_{H_3O^+}$ and c_{OH^-} are the concentrations of hydronium and hydroxide ions, respectively. Hence, the amount of ions in pure water is very small. Note, that K_w is strongly temperature dependent [16].

Aqueous hydronium ions are strongly hydrated with a hydration enthalpy of -1091 kJ/mol [17]. The average number of water molecules in the first hydration shell has been investigated via various experimental and theoretical methods and values between three and seven have been proposed [18, 19]. The hydroxide ion, on the other hand, has a hydration enthalpy of roughly -460 kJ/mol [17] and to current understanding, its hydration structure is different from that of the hydronium ion. It seems to interact weaker with the surrounding water molecules, as it does not donate hydrogen bonds [20, 21]. The two self-ionization products of water thus show different bulk hydration behaviors, which is likely to affect their respective behavior at the water-vapor interface. This is currently an intensely debated and investigated issue [5–7, 22].

2.2 Properties of aqueous solutions

A solution is a mixture of two or more components that are usually divided into solutes and solvents. The only solvent used in this thesis is water, while various different types of solutes, e.g. atomic ions, organic ions, organic acids, inorganic ions etc., are investigated. The following text introduces briefly the major properties of aqueous solutions. More details can be found in pertinent textbooks, such as references 23–25. After an overview on important interactions in solutions and the general concepts of equilibria, specific properties of ions and molecules in solutions are discussed.

Interactions in solutions

The interactions between solutes and water molecules in an aqueous solution are usually on the order of or stronger than the interactions between solutes in solution. Electrostatic interactions such as ion-dipole, dipole-dipole, ion-

induced, and dipole-induced forces govern the interactions of solutes and solvent species in mixtures. The weaker van der Waals forces are dominant between non-polar species and are very short-ranged. The strongest interactions are formed between ionic species and water, where water molecules arrange around the ions, forming rather structured hydration shells. A special type of dipole-dipole interaction is known as hydrogen bonding and plays an essential role in aqueous systems, as it enables the water molecules to dissolve other polar compounds. Induced forces are weaker than the previously described forces and arise from ions or dipoles that distort the electron distribution of a nearby non-polar compound.

Concentrations and solubility

Concentration is the abundance of a compound in a solution, which can be specified in various ways. Most commonly used in the context of solution chemistry are concentrations of a solute given as number of moles per volume solution, which is referred to as molarity, in [mol/dm^3] (M), or per mass solvent, which is referred to as molality, in [mol/kg H_2O] (m). Since mass is independent of temperature, molal concentrations are temperature-independent. Furthermore, unlike volumes, masses are additive and possible intermixing volumes do not need to be taken into account. Molality is the preferred representation of concentrations, especially when temperature changes and thereby density changes are expected to play an important role. On the other hand, as molarity is a type of number density, results from XPS studies can more easily be related to molar concentrations, which will be discussed in more detail in section 4.5.2. Concentrations can also be given as the ratio of solute to solvent, as e.g. mass or mole fraction. The mole fraction x of a solute is the ratio of solute moles and the sum of solvent and solute moles.

Solubility of a solute is the maximum amount that can be dissolved in a certain quantity of solvent. Solubilities may strongly depend on temperature or co-dissolution of other species. Generally, ionic and polar species can be dissolved easily in water. If parts of a compound are hydrophobic, i.e. repelled by water, its solubility in water is reduced. The saturation concentration, where a maximum of solute is dissolved, is often given as mass or moles per volume solution and can be found tabulated in literature, e.g. reference 16.

The ability of a compound to evaporate is also referred to as its volatility, which is also temperature dependent. In solutions, the solute evaporates proportionally to the relative dissolved amount. The relation between partial pressure of a solute above a solution, i.e. the amount of compound in the gaseous phase, and the concentration of the solution is expressed in the so-called Henry's law, where k_H is the Henry's law constant, see equation 2.2 [24].

$$c_{\text{solution}} = k_H \cdot p_{\text{gas}} \tag{2.2}$$

The Henry's law constant is specific for each solute-solvent pair at a given temperature, and are strictly speaking only valid for dilute solutions. As a so-

lution becomes more concentrated, the gaseous concentration becomes similar to the pure compound's vapor pressure instead.

Chemical equilibria and equilibrium law
Chemical equilibria are dynamic, i.e. there is a forward and backward reaction. For a certain set of concentrations of the product and reactant the equilibrium will adapt. The characteristic equilibrium constant K_c for the reaction of the compounds A and B to form C and D:

$$\mathrm{A} + \mathrm{B} \rightleftharpoons \mathrm{C} + \mathrm{D}, \tag{2.3}$$

is given as

$$K_c = \frac{c_\mathrm{C} \cdot c_\mathrm{D}}{c_\mathrm{A} \cdot c_\mathrm{B}}. \tag{2.4}$$

The concentrations of the reactants and products are c_A, c_B, c_C and c_D, respectively. Equation 2.4 is also known as the law of mass action and describes the equilibria conditions of a chemical reaction at constant temperature.

A well-known law in chemistry is the *equilibrium law*, or also called *Le Châtelier's principle* [25], which can be used to explain how a system reacts to e.g. changed conditions. In simple terms it says, that if the external conditions of a system are changed, the system reacts by shifting the equilibrium such that the effect of the conditions are minimized. For example, if a substance A is added to the equilibrated system given in equation 2.3, the equilibrium is shifted to the right side, as A is increasingly consumed by that.

2.2.1 Aqueous solutions of electrolytes

Electrolyte salts dissociate when dissolved in water, creating ions of opposite charges. This is mainly a consequence of the high dielectric constant of water [26], which promotes the dissociation of ionic compounds. As their charges are effectively screened, the attractive forces between the oppositely charged ions are increasingly reduced. The formation of hydration shells around the dissociated ions reduces the system's energy and maximizes the ion-water interactions. The strength of hydration, resulting from the number of directly bound water molecules and bond distance, may depend on various parameters, such as shape, size and charge state of the ion [27–29]. A hydration shell consists of water molecules that orient themselves around an ion, turning their polar partial charges towards the opposite charged ion, as it is depicted in figure 2.1. Is the charge of the ion not sufficiently screened by the first water shell, more weaker bound hydration shells may be formed. Solutions in equilibrium are usually considered as homogeneous, at least in the bulk. But on molecular-scale, the local surroundings of a species can be of inhomogeneous character, which is usually described by asymmetric hydration shells. The

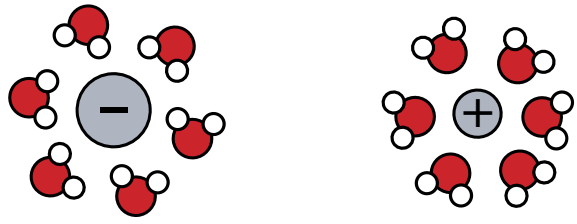

Figure 2.1. The first hydration shell of a negatively and a positively charged ion. The partially negatively charged oxygen atoms of the water molecules point towards the positive ion, while the partially positively charged hydrogen atoms of a water molecules direct towards the negative ion.

above given general rules for chemical equilibria can also be applied to reactions involving ionic species, which are strictly speaking only valid for *ideal* solutions or solutions in which interactions between the dissolved compounds can be neglected. For the dissociation of a compound BA in aqueous solution with concentration c_{BA}, the condition for equilibrium is given in equation 2.5, where c_{B^+} and c_{A^-} are the concentrations of the ions B^+ and A^-, respectively.

$$\mathrm{BA} \rightleftharpoons \mathrm{B}^+ + \mathrm{A}^- \qquad \text{with} \qquad K_{\mathrm{D}} = \frac{c_{\mathrm{B}^+} \cdot c_{\mathrm{A}^-}}{c_{\mathrm{BA}}} \tag{2.5}$$

K_D is is also referred to as stoichiometric dissociation constant. The law of mass action can only be used for low concentrations (< 0.1 mol/dm^3) of electrolytes. The main reason for this is that at elevated concentrations the attractive and repulsive forces between the solutes can no longer be neglected. The attractive forces appear as if the concentration of the solute was lower than it actually is, yielding a higher concentration of undissociated molecules (see equation 2.5). To be able to apply the law of mass action even to *real* solutions, the physical chemist G. N. Lewis introduced the concept of activity [30]. The idea is to convert the actual ionic concentration c into the effective activity a by multiplying the concentration with a correction factor that is usually called activity coefficient γ. The activities can then be used instead of concentrations in equation 2.5 to determine the thermodynamic dissociation constant K_D for non-ideal systems.

$$a = \gamma \cdot c \tag{2.6}$$

There are different models to determine activity coefficients. Hückel and Debye proposed an equation for electrolyte solutions with ionic strength of less than 0.1 mol/dm^3 [25]. Ionic strength is a commonly used measure for ions in a solution and is calculated using equation 2.7, where z_i and c_i is the charge and concentration of the i$^{\mathrm{th}}$ ionic species in solution, respectively.

$$I = \frac{1}{2} \sum_i z_i^2 \cdot c_i \tag{2.7}$$

The activity coefficient γ_i of an ion with charge z_i can be determined according to Hückel and Debye as follows:

$$\log \gamma_i = -\frac{1}{2} \cdot \frac{z_i^2 \cdot \sqrt{I}}{1+\sqrt{I}}. \tag{2.8}$$

If the ionic strength of a solution is increased by, e.g. the addition of salt to the solution, the activity coefficients are reduced, see equation 2.8. This leads to decreased activities of the ions a_{B^+}, a_{A^-}, see equation 2.6. According to the law of mass action, this results in a decreased activity of the undissociated molecules. Hence, the degree of dissociation decreases with increasing ionic strength.

There are more advanced models to estimate activity coefficients, which are based on thermodynamic properties of the different species. In atmospheric science commonly used models are the *UNIFAC* (UNIversal quasi-chemical Functional group Activity Coefficients) [31, 32] and E-AIM (Extended - Aerosol Inorganics Model) models [33]. The UNIFAC model makes use of the contributions of the various functional groups of the compounds in solution and their interactions to estimate activity coefficients. It is a semi-empirical model, which is developed to describe non-electrolyte solutes in aqueous solutions. The E-AIM model, on the other hand, can be used for both molecular and ionic species and even mixed solutions. The calculation of acitivity constants via the E-AIM model is based on equilibrium constants for phase transitions and thermodynamic equations.

Ion-pairing

Ions of opposite charge can come very close together in a solution and form so-called ion-pairs [34]. The resulting pairs of such a process, which is also referred to as ion-association, are often classified into contact ion-pairs, solvent-shared or solvent-separated ion-pairs. The natural attraction of oppositely charged species due to electrostatic forces is somewhat reduced in the aqueous environment, because of the surrounding solvent that screens part of the charges. Ion-association is generally favored in solvents with a low dielectric constant and between highly charged or small ions. For example, sodium chloride in water does not exhibit ion-pairs to any appreciable extent, except for very high concentrations. Sodium and sulfate ions, on the other hand, have been found to form a considerable amount of ion-pairs in solution [35].

2.2.2 Aqueous solutions of organic molecules

Molecular solutes mostly interact with water by van der Waals forces and, depending on their functional groups, by hydrogen bonding [24]. In this thesis mostly organic molecules are investigated, i.e. carbon-containing compounds with polar functional groups, e.g. alcohols or carboxylic acids. Such

species usually have hydrophobic and hydrophilic parts and their relative size and strength contributes to the overall hydration structure and behavior of the molecule in solution. These molecules are also called amphiphiles, as they can bind strongly with their hydrophilic parts to the solvent water and are therefore still miscible with water. The hydrophobic parts lead to a loss in solvent-solvent interactions. The hydrating water molecules form cavities within the dielectric medium around these molecules [36], where water-water hydrogen bonds are broken to accommodate the hydrophobic part of the solute. The hydrophilic parts, on the other hand, possess polar or even ionic character and interact strongly with water, possibly forming strong hydrogen bonds. The hydrophobic parts of amphiphiles may aggregate and form micelles or adsorb at other hydrophobic interfaces. The described dual properties allow for example soap molecules to dissolve very hydrophobic species such as oil in water. In biochemistry, amphiphilic molecules enable the connection between hydrophobic-hydrophilic interfaces, which can be found e.g. between lipid layers in aqueous environments, and thereby play a crucial role for their function.

Organic acids and bases

Organic acids and bases are compounds that contain titratable functional groups, such as carboxylic acid, amino or phosphate groups, that may accept or donate protons. An ionic conjugate is formed that is stable in the aqueous environment in contrast to the gaseous phase, where these kind of reactions are suppressed. The dissociation of acids or bases respectively, see equation 2.9, can be quantified by applying the law of mass action. The equilibrium constant for the dissociation reaction is given as K_a.

$$\mathrm{HA} + \mathrm{H_2O} \rightleftharpoons \mathrm{H_3O^+} + \mathrm{A^-} \qquad \text{with} \qquad K_\mathrm{a} = \frac{c_{\mathrm{H_3O^+}} \cdot c_{\mathrm{A^-}}}{c_{\mathrm{HA}}} \tag{2.9}$$

As the acid HA always dissociates into equal amounts of $\mathrm{H_3O^+}$ and $\mathrm{A^-}$, the concentration of the conjugated base is equal to the concentration of hydronium ions, $c_{\mathrm{A^-}} = c_{\mathrm{H_3O^+}}$. After dissociation the acid's concentration can be computed as follows: $c_{\mathrm{HA}} = c_{\mathrm{HA_{tot}}} - c_{\mathrm{H_3O^+}}$ and the hydronium concentration $c_{\mathrm{H_3O^+}}$ can be determined using equation 2.10.

$$c_{\mathrm{H_3O^+}} = -\frac{K_\mathrm{a}}{2} + \sqrt{\left(\frac{K_\mathrm{a}}{2}\right)^2 + K_\mathrm{a} \cdot c_{\mathrm{HA}}} \tag{2.10}$$

The negative logarithm of the hydronium concentration gives the pH of the solution, see equation 2.11.

$$\mathrm{pH} = -\log c_{\mathrm{H_3O^+}} \tag{2.11}$$

Using the approximation that $c_{\mathrm{HA}} = c_{\mathrm{HA_{tot}}}$, which should only be used for low $c_{\mathrm{H_3O^+}}$, equation 2.10 simplifies to the following equation, which is also known

as Hendersen-Hasselbalch equation [25, 37].

$$\mathrm{pH} = \mathrm{p}K_\mathrm{a} + log\left(\frac{c_\mathrm{HA}}{c_{\mathrm{A}^-}}\right) \tag{2.12}$$

For the case of equal amounts of acid and conjugated base form, the hydronium concentration is equal to the dissociation constant $K_\mathrm{a} = 10^{-\mathrm{p}K_\mathrm{a}}$.

2.3 Interfacial phenomena

With the major principles of bulk chemistry briefly introduced, in the remainder of this chapter a few concepts used to describe the air-water interface of a solution are summarized. Approaching the boundary between two phases, forces acting on residing species may deviate increasingly from those prevailing in the bulk of the solution. Species with a high propensity to reside at the surface can be described as surface-active. Such species tend to accumulate at the water-vapor interface, which results in a lowered surface tension of the solution as compared with that of pure water. This may alter the spatial distribution of solutes in the interfacial region drastically. In the following subsections known surface related properties and their theoretical descriptions are discussed.

Surface tension

Surface tension, as viewed from a mechanical point of view, is given in terms of a force exerted in the surface plane per unit length. From a thermodynamic perspective, surface tension is defined as the excess free energy due to the presence of a surface. These two concepts are combinable and surface tension σ can be expressed as the work W or energy necessary to change the surface area A, $\sigma = \frac{dW}{dA}$. The most commonly used units are Newton per meter [Nm^{-1}]. Surface tension makes liquid droplets forming spheres, because this shape yields the smallest surface-to-volume ratio.

As described above, surface tension can also be expressed as the energy change associated with expanding the surface area, which increases the amount of species in the surface region. J.W. Gibbs posted a formalism, which relates the surface tension of a solution to the excess amount of solute per surface area Γ_i with the chemical potential of the i^{th} component μ_i.

$$\Gamma_i = -\left(\frac{d\sigma}{d\mu_i}\right)_{T,\mu_{i\neq j}} \tag{2.13}$$

Equation 2.13, which is also referred to as the Gibbs isotherm [23], shows that with a net positive surface excess concentration, surface tension is decreased as compared to no surface excess. In other words, for solutes that are depleted

in the surface region, surface tension should increase, as it is known for e.g. electrolyte solutions.

The origin of surface tension lies in microscopic molecular interactions. Molecules at the boundary between liquid and vapor phase have less neighbors, hence they are therefore in a higher state of energy and the strength and nature of the interactions with the remaining dimensions become more important.

Besides the experimental techniques, various models have been proposed to approximate surface tension for aqueous solutions. For example the semi-empirical Szyszkowski equation [38] or the thermodynamic-based one proposed by Sprow and Prausnitz [39, 40], who used Gibbs free energy and the different concentrations in the surface and the bulk sample for an equilibrated system. The latter was further used by Li et al. [41] for electrolyte solutions and is applied in paper I and V in this thesis.

Langmuir adsorption

Surface-active solutes can reside in the surface region, which can be expressed in a degree of coverage. The coverage of a surface is usually given as a fraction of occupied adsorption sites and free available sites. Changes in coverage as a function of concentration of a solution at given temperature is also called an adsorption isotherm. The most commonly used adsorption model is the one proposed by I. Langmuir, which is built upon a few major assumptions, including specific but identical surface adsorption sites, coverage-independent adsorption energy and formation of a monolayer [38]. These conditions are rarely fulfilled by *real* systems, especially the adsorption energy is likely to depend on the degree of coverage. Because at a high degree of coverage, cooperative effects, such as lateral interactions between adsorbed molecules, may contribute strongly to the energy balance and change thereby the adsorption process locally. This is also subject of paper III. Despite the limiting assumptions of the Langmuir model, it provides a satisfying first approximation that helps to compare the adsorption behavior of different solutes and quantify their interactions with water to a first approximation. A few extensions of the Langmuir model are proposed, attempting to incorporate the limitations set by the above mentioned assumptions [38, 42].

2.3.1 Atmospheric chemistry

Studies of surface phenomena, including dissociation of acids or bases, spatial distribution of compounds in the surface region and relative enrichment are presented in this thesis. A few of the studied aqueous systems were chosen mainly due to their important role in atmospheric chemistry. Starting from the planning until the discussion of results of the XPS experiments, the impact of the results on the behavior of atmospheric nanoparticles and cloud physics in

general was discussed. In particular parameters that may be strongly affected by changes in the surface composition and structure, such as vapor pressure, surface tension or reactivity were considered. In the following subsections, a few important concepts of atmospheric systems are introduced. Detailed information and derivations of the given equations can be found in textbooks, e.g. references 23 and 43.

Kelvin equation

Cloud droplets are formed by condensation of vapors. Even though relative humidity exceeds 100 %, condensation does not occur directly, as it requires an overload of saturation to form droplets. The level of relative humidity above 100 % is often referred to as supersaturation. The Kelvin effect originates from the surface curvatures that increases the particles vapor pressure. The greater vapor pressure over a curved surface p_r with radius r, compared to the vapor pressure over a plane surface p_∞ has been theoretically derived by W. Thomson and is usually referred to as the Kelvin equation, see equation 2.14 [23].

$$\ln\left(\frac{p_r}{p_\infty}\right) = \frac{2\sigma m}{\rho_l R T r} \tag{2.14}$$

Here m is the molecular weight, ρ_l the density of the liquid, R the gas constant and T the absolute temperature.

Particles containing hygroscopic matter, particularly inorganic salts, are very efficient in absorbing water from the vapor phase already at very low relative humidity. This prevents the water from evaporating, thus counteracting the increased vapor pressure due to the curvature effect to some extent. The combination of these two effects is called Köhler theory and is described below.

Köhler theory

With Köhler theory one can predict the conditions under which water vapor condensates and starts the formation of cloud droplets. The theory was first developed by H. Köhler [44].

In classic Köhler theory the relative humidity (RH) or supersaturation S, that is needed for a droplet to grow, is mathematically described by equation 2.15.

$$S = a_w \exp\left(\frac{4\sigma M_w}{RT\rho_w D}\right) \tag{2.15}$$

Here, a_w is the water activity of water in solution and is part of the Raoult term. The density and molecular weight of water is denoted as ρ_w and M_w, respectively. D is the diameter of the droplet. As the relative humidity increases, cloud droplets grow until a so-called critical supersaturation, S_{crit} is reached. That point corresponds to a critical diameter, d_{crit}, and is where the particle is considered to be *activated* into a cloud droplet, which means that it can theoretically grow spontaneously, if $S > S_{\text{crit}}$, see figure 2.2. To derive the Köhler

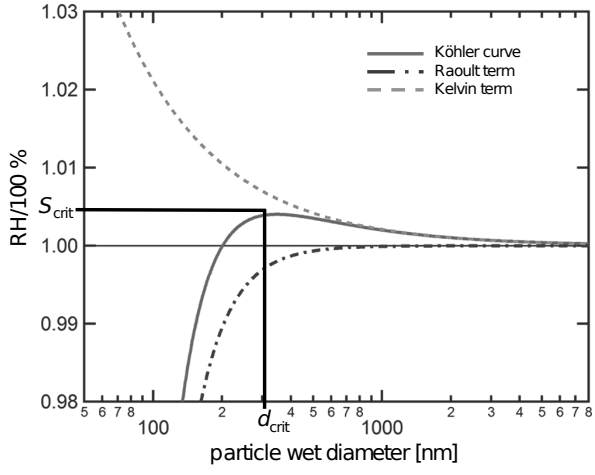

Figure 2.2. Example of a Köhler curve for an ammonium sulfate particle with intial dry diameter of 50 nm. The Kelvin contribution and the Raoult term are also shown as a function of the particle's wet diameter. Adapted with permission from [46]. Copyright 2015 American Chemical Society.

equation, the Kelvin equation (equation 2.14) and the modified Raoult's law, which defines the water equilibrium over a flat aqueous mixture, are combined, see equation 2.15 [45]. S_{crit} and d_{crit} depend on the composition and structure of the aerosol particle. Solubility of the chemical compounds and the dry particle's diameter are decisive parameters, which affect the shape of the resulting Köhler curve [46].

Simply speaking, the water activity term (Raoult term) describes the ability of solutes to lower S_{crit} while the exponential term (Kelvin term) takes the increased saturation, due to the curvature effect, into account. Both effects approach 1 for high particle diameters, the Raoult term from below and the Kelvin term from above. In figure 2.2 an example of a Köhler curve for an ammonium sulfate particle with initial dry diameter of 50 nm is shown. It can be seen that the importance of the Kelvin contribution over the Raoult contribution increases with increasing particle diameter. For very big particles the curve approaches the Kelvin contribution and the solute contribution becomes so small that the droplet mostly behaves like a pure water particle [46].

This classic version of the Köhler equation only describes binary mixtures. To include for example effects of multi-component systems and also allow the addition of organics or size-dependent modulations of the surface tension and particle content, modifications to this theory have been proposed [47–51].

3. Basic concepts of X-ray photoelectron spectroscopy

Synchrotron-based XPS on a liquid micro-jet is the main experimental tool in this thesis, utilized to provide microscopic insights into aqueous surfaces. The aim of this chapter is to give an overview on major aspects of the XPS method and its application. More detailed information on the technique can be found in e.g. references 52 and 53

3.1 Major principle of core-level spectroscopy

XPS is the measurement of the kinetic energy of emitted electrons from gases, solids or liquids due to the photoelectric effect [54]. The sample is irradiated by photons with well-known energy $h\nu$, leading to the emission of an electron if the incident photon energy is higher than the binding energy (BE) of the electron's electronic state in the sample. The excess photon energy defines the kinetic energy of the emitted electron E_{kin} and it can be stated that:

$$h\nu = \mathrm{BE} + E_{\mathrm{kin}}. \tag{3.1}$$

If the energy of the photons is precisely known, and by measuring the kinetic energy of the photoelectrons, binding energies of electrons in atoms thus can be computed easily. To obtain a PE spectrum, the number of emitted electrons is measured as a function of kinetic energy for a given photon energy. This method comprises an unique combination of features being both element specific and surface sensitive and it is used in different research fields to probe e.g. atoms, molecules and condensed matter in vacuum. This technique is also referred to as Electron Spectroscopy for Chemical Analysis (ESCA), which was developed by K. Siegbahn and co-workers [55], for which he received the Nobel Prize in physics in 1981.

3.2 Element sensitivity and chemical shift

XPS can be applied to core-level orbitals or valence levels. Core-level spectroscopy is particularly useful for chemical analysis of a sample, due to the characteristic binding energies of inner shell electrons, which have in first approximation mostly atomic orbital character. Thus, based on the unique binding energy of a core electron [56], each element in a sample can be identified.

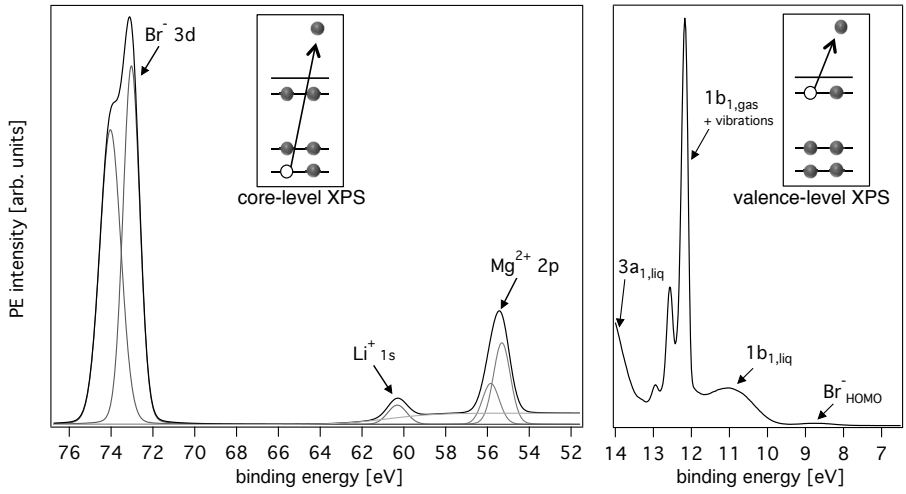

Figure 3.1. The basic concept of core- and valence-level photoionization are depicted as insets into example spectra of an aqueous solution containing LiBr and $MgBr_2$. The spectra are recorded with a photon energy of 150 eV. From the spectrum on the left, Li^+, Mg^{2+} and Br^- can be easily identified. The valence spectrum (right side) shows mainly valence orbitals of water and its vibrations as well as the highest occupied molecular orbital level of Br^-.

Valence-level electrons, on the other hand, are usually more delocalized and can participate in chemical bonding. Thus valence levels are more of molecular orbital character, with lower binding energies than core-level electrons. In figure 3.1 the basic concepts of valence and core-level photoionzation are depicted together with examples of XPS spectra from an aqueous solution containing LiBr and $MgBr_2$. The exact binding energy of a core-level of an atom in a sample depends on the chemical state and the direct surroundings of the atom. The shift of binding energies of one specific chemical state versus the binding energy of the pure element is referred to as the chemical shift, which allows the discrimination between equivalent atoms with different chemical surroundings or in different phases of matter, such as solid, gas or liquid. More specifically, the relative withdrawal power of neighboring atoms determine the extent of the resulting shift. An electron-withdrawing atom or functional group, e.g. oxygen or hydroxyl group, attached to a carbon atom reduces its local electron density, which results in a less effective shielding of the carbon atom's nucleus and causes the core-electrons to be more tightly bound. Examples illustrating the chemical shift for the same core-level in different chemical environments can be found in the different papers included in this thesis. Due to the chemical shift, it is for example possible to discriminate between different protonation states of a carboxylic acid or amine, which yields one of the greatest advantages of the XPS method over other surface-sensitive experimental techniques. Note, that core-level binding energies of anions shift

towards lower binding energies in comparison with the same species in neutral form, while the binding energies of cations are shifted to higher values. Furthermore, a core-level electron originating from a molecule in the gaseous phase has usually a higher binding energy compared to the same molecule in solid or liquid phase.

3.3 Binding energy and PE lines

A common definition of the binding energy of an electron in an atom or molecule is the negative energy of the atomic or molecular orbital accommodating this electron. This only holds if no relaxation processes take place after the ionization. When an electron is emitted, the remaining electrons will try to minimize their energy. Relaxation processes will take place, which are usually referred to as final-state effects. In more general terms, the binding energy of an electron can be expressed as the energy difference between the initial state E_i and the final state E_f of the system, see equation 3.2 [52]. This corresponds to the energy difference between the neutral atom with n electrons and the charged ion with $n-1$ electrons.

$$BE = E_f(n-1) - E_i(n) \tag{3.2}$$

As said before, if no relaxation processes take place, i.e. electronic rearrangements following the photoemission process, this binding energy would be equal to the negative energy of an atomic or molecular orbital accommodating this electron. This approximation is known as Koopman's theorem [57] or frozen orbital approximation, and it can only be considered as a first approximation. Final-state effects have to be taken into account, especially in condensed samples for a more precise analysis, since the ionization of an electron in an orbital affects other orbitals in the surroundings strongly. The binding energies obtained from these experiments contain therefore both information about the binding energy of the electron in the initial state and the relaxation of the system after emission of a photoelectron.

The lifetime τ of a hole in an orbital, i.e. an empty electron spot created by the ionization process, is the time it takes for the system to fill that hole with an electron and/or relax from excited states. The energy of the orbitals cannot be known accurately, due to Heisenberg's uncertainty principle, resulting in a broadening of the PE line width, see equation 3.3 [58].

$$\delta E \approx \frac{\hbar}{\tau} \tag{3.3}$$

The finite lifetime results in a Lorentzian-like spectral line shape. For a given element, the value for the line width broadening due to the lifetime is typically larger for inner-shell orbitals compared to outer-shell orbitals. This is because

an inner-shell hole can be filled with an electron from an outer-shell orbital quickly, while vacancies in outer-shell orbitals can generally live longer. The Lorentzian full width at half maximum (FWHM) of N1s, C1s and S2p core levels, which are core-levels that are investigated in this thesis, are found to be approximately 0.13, 0.10 and 0.05 eV, respectively [59].

Additionally, PE lines are broadened due to intrinsic factors like vibrations within the molecules and instrumental effects, e.g. energy spread of the incident X-rays and resolution of the electron energy analyzer. It is typically assumed that these contributions to the PE peak have a Gaussian line shape. Especially for the case of liquid samples, line width broadening due to vibrations of the atoms and molecules and their interactions with the solvent dominate greatly over lifetime induced broadening.

3.4 Surface sensitivity

Photoelectron spectroscopy applied to condensed matter yields an inherent surface sensitivity, which originates from the short distance that the emitted electrons can travel inside the sample without loosing energy. As depicted in figure 3.2, ionizing X-rays can penetrate samples far into the bulk, depending on their energy. But ejected electrons from bulk atoms loose their energy in inelastic collisions with atoms of the bulk material. Electrons that are ejected from surface or surface-near atoms, on the other hand, can leave the condensed sample directly or after only a short distance, see figure 3.2. The probability of inelastic scattering and energy loss is thus very low.

There are different measures to express the surface sensitivity of XPS. The terms *inelastic mean free path*, *effective attenuation length* (EAL) and *mean escape depth* are the most commonly used, but are not interchangeable concepts. The EAL is a commonly used concept, which gives the shortest travel

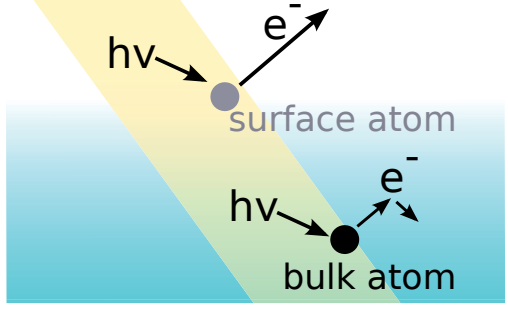

Figure 3.2. Impinging X-rays penetrate far into a sample and electrons are ejected along the path. Emitted photoelectrons from a bulk atom loose quickly their energy via inelastic collisions with the neighboring atoms, while a photoelectron emitted from a surface atom can leave the condensed sample and is subsequently detectable.

distance between two points in which the initial electron signal is reduced to 1/e [60]. It is mainly used in this thesis to quantify the degree of surface sensitivity.

The EAL changes considerably as function of kinetic energy of the photoelectrons. Up to a certain accuracy, a striking generality in this behavior obtained from different materials led to the *universal curve* for electrons in condensed matter. This curve has mainly been obtained for metals but can potentially be used for other condensed materials. Between 50 and 150 eV kinetic energy the electrons EAL is shortest, resulting in a high surface contribution to the recorded intensities. The EAL gradually increases for higher kinetic energies and the sample's bulk contributes more to the recorded intensities. This effect is often utilized for depth-profiling experiments, where the photon energy is varied. This changes the kinetic energy of the outgoing photoelectron, resulting in a variation of the relative amounts of signal originating from bulk and surface of the sample.

For aqueous samples this curve is only poorly known. Important work on this subject has been provided by e.g. references 61–64, where the minimum of the universal curve for aqueous solutions is estimated to be in the order of 1 nm for a liquid micro-jet.

3.4.1 Photoionization cross-section

The photoionization differential cross-section is dependent on the energy of the incoming photons, the material and orbital of interest. In the dipole approximation, it is expressed as a function of the angle between the direction of the ejected electron and the polarization of the incoming photons, and characterized by a so-called asymmetry parameter β [65]. The β parameter generally depends on the ionized orbital and the photon energy. It accounts for the anisotropic intensity emission patterns of the photoelectrons, which arises from angular momentum conservation in the photoionization process. For a certain angle between the polarization direction of X-rays and the direction of outgoing electrons, the photoelectron intensity is approximately the same for all orbitals, i.e. independent of β. No corrections, in first approximation, for angular distributions have to be implemented for XPS spectra obtained at this angle, which is usually referred to as the *magic angle* with 54.7° [52, 66, 67].

When comparing PE lines originating from the same atomic orbital but in different chemical surroundings, it is often assumed that the photoionization cross-section is essentially unchanged, i.e. the molecular composition does not significantly alter the PE intensity at a given kinetic energy. Nevertheless, the alteration of the photoionization cross-section as function of kinetic energy of the outgoing electrons has been studied for various molecules in the gaseous and liquid phase recently, and energy-dependent, non-stoichiometric PE intensity oscillations have been found [64, 68, 69]. The origin of this modulation

is assigned to scattering of the outgoing electrons on neighboring atoms and are strongest within up to 200 eV above the ionization threshold. As this effect is strong even well above the ionization threshold and observed also in liquid matter, it should be taken into account when deducing information on stoichiometry or molecular orientation in probed samples.

3.5 Electron energy analyzer

X-rays illuminate a sample causing electrons to be emitted with a range of energies and directions. Electron optics, usually consisting of a set of electrostatic lenses, are used to collect a portion of these emitted electrons and focus them onto the entrance slit of a hemispherical analyzer. Inside the hemispherical analyzer, electrostatic fields ensure that only electrons with a given kinetic energy, the so-called pass energy, can arrive in the middle of the detector. By setting voltages on the focusing lenses, electrons of a specific kinetic energy are not only focused onto the entrance slit of the hemispherical analyzer, but are also decelerated or accelerated from their initial energy so that their kinetic energy after passing through the entrance slit, matches the pass energy of the hemispherical analyzer. A spectrum is recorded by scanning the voltages applied to the focusing lenses. An energy step size and a suitable dwell time are chosen and the number of electrons hitting the detector is recorded as a function of the electron's kinetic energy. Since the kinetic energy increases with decreasing binding energy for a given photon energy, a PE spectrum is typically presented with the binding energy on the x-axis evolving from right to left for higher energies.

3.5.1 Resolution

Instrumental energy resolution δE, is determined by the entrance slit width s, the pass energy E_p and the diameter of the electron energy analyzer d, as given in equation 3.4.

$$\delta E = \frac{s \cdot E_p}{d} \tag{3.4}$$

That means, the best resolution for a certain electron energy analyzer is obtained when a small slit is used together with a low pass energy. Both these parameters are proportional to the PE intensity, thus a compromise must be found. Additional to the instrumental broadening and lifetime broadening, which is described above, broadening contributions from the photon source, temperature and from the sample itself are included in the final PE line width.

3.6 Photon source

Synchrotron radiation is electromagnetic radiation emitted by charged particles, usually electrons, that are accelerated perpendicular to their direction of motion. Electron storage rings are used to store bunches of electrons, which circulate inside an evacuated tube. Bending magnets, which are situated at the bending points of the storage ring, produce broad bremsstrahlung, while insertion devices, such as undulators and wigglers, are installed on the straight sections of the storage ring. Insertion devices consist of a periodic structure of dipole magnets that force electrons to an oscillating motion when passing through. By changing the distance of the dipole magnets vertically, the so-called undulator gap, the distribution of energy of the produced photons can be changed. The generated light is brought to the user via so-called beamlines. A focusing mirror is used to direct the X-rays towards a monochromator, which selects a narrow band of wavelengths of the produced radiation. The exit slit of the monochromator and the monochromator grating determine the resolution. A final refocusing mirror can be used to adjust the photon beam before it enters the experimental chamber.

Synchrotrons are the most commonly used light sources for X-ray and ultraviolet (UV)-based spectroscopy methods, which have beneficial properties, such as high photon flux and tunable photon energy at high brilliance for a wide range of energies. Users, who have successfully applied for experimental time, are provided with a large range of wavelengths to choose between. Such radiation sources are large research facilities, which can be found in many countries, while all experiments that were performed for this thesis, took place at the Swedish national synchrotron, MAX-lab, in Lund at the MAX-II ring. Besides synchrotrons, X-ray tubes, gas discharge lamps and laser setups can be used as X-ray sources in home-laboratories. These are usually restricted to certain photon energies.

4. XPS on a liquid micro-jet: practical aspects and challenges

While XPS is a powerful tool to study various materials, the restriction to vacuum remains a challenging task. Due to the short escape depth of photoelectrons at low kinetic energies and the considerably larger absorption of photons in the vapor phase around a volatile surface, experiments must meet conditions with low background pressure by minimum evaporation and efficient differential pumping. Furthermore, X-ray radiation can cause sample damage, i.e. decomposing molecules, and liquid water freezes quickly in vacuum due to strong evaporative cooling. To meet these requirements and enable the application of XPS on liquid samples, advances have been made in the last fifty years, elegantly overcoming these challenges. In this chapter, a quick time-line on major historical progresses is followed by a description of the experimental setup used for the investigations discussed in this thesis. This chapter includes also a detailed description of sample preparation and data treatment. A short summary on information that can be obtained from XPS results of aqueous samples concludes this chapter.

Historical Advances

The pioneers in the field of XPS on liquid surfaces are K. Siegbahn and co-workers. In their first reported work, they studied liquid formamide and demonstrated the complete separation of the gaseous and the liquid phase PE signal. The binding energies were evaluated and reported in "ESCA applied to liquids" by K. Siegbahn and H. Siegbahn in 1973 [9]. As the quick loss of energy of photoelectrons in dense vapor or condensed phases require the experiment to be performed in vacuum, highly volatile compounds, such as pure water with a vapor pressure of 23.3 mbar [16], seem inappropriate samples at first. K. and H. Siegbahn performed XPS experiments on either liquids with very low vapor pressures or concentrated aqueous electrolyte solutions, where the background pressure is reduced to a minimum [70]. These studies were conducted on a liquid floating over a rotating disc, which yields a continuously renewed sample. A few years later, M. Faubel and co-workers proposed a new approach that would allow the probing of even more volatile liquids, such as water, utilizing a liquid micro-jet [10]. Using this technique, the liquid is pushed through a glass nozzle with high backing pressure, forming a thin jet (a few micrometers thick) that is injected into an evacuated chamber. As the liquid micro-jet is traveling with high speed, the sample is continuously refreshed and thus free from contamination or beam damage. The small

amounts of liquid that is injected into the experimental chamber results in only a minimum increase in background pressure, which enables the detection of PE signal from the liquid and the gaseous phase.

4.1 Experimental setup at beamline I411, MAX-lab

Most XPS experiments presented in this thesis were conducted at the undulator beam line I411 [71, 72] at the Swedish national synchrotron facility, MAX-lab in Lund. It is equipped with a permanent multi-purpose end station, where gas, liquid and solid samples can be investigated. The beamline delivers photons with energies in the range from 50 to 1000 eV, but only up to roughly 600 eV with reasonable photon flux for studies on a liquid micro-jet.

A high resolution Scienta R4000 hemispherical electron energy analyzer is attached to the main experimental chamber and is usually operated using a 500 μm, curved entrance slit for PE experiments. The energy resolution is better than 0.25 eV at pass energies of 100 to 200 eV. The detection system contains two multi-channel plate detectors and a fluorescence screen together with a CCD camera. Angle resolved measurements can be performed as the main chamber can be rotated around the axis of the incoming photon beam. All experiments performed for this thesis were conducted with the propagation direction of the liquid jet perpendicular to the photon beam. The detection axis of the electron spectrometer was at an angle of 54.7° relative to the plane of polarization of the photon beam, the so-called magic angle, see section 3.4.1.

To shield and retain the detection system situated in the hemisphere from breaking and to maintain the vacuum in the beamline close to the endstation at low pressures, an additional differentially pumped stage is inserted into the main chamber. This stage has an opening for the X-rays to enter and a skimmer is attached at 90° with respect to the incoming X-ray beam. In the jet's stream direction a cooling trap is attached to catch remains of the liquid sample and freeze them. For alignment, the differentially pumped stage can be rotated and moved up or down. A sketch of the setup at MAX-lab is shown in figure 4.1 and photographs of the same are shown in figure 4.2. Similar setups are operational at e.g. Bessy II in Berlin (Germany) [73], LNLS in Campinas, Brasil, ALS in Berkeley, USA [74], SOLEIL in Paris, France, or at SLS in Villingen, Switzerland [75].

As discussed above, the collision-free travel to the entrance of the hemispherical electron energy analyzer is of great importance for the correct kinetic energy detection of the photoelectrons emitted from the liquid surface. Passing the entrance skimmer, electrons are guided by electrostatic lenses in high vacuum, where the loss of energy is negligible. The path through the dense water vapor around the jet should be as short as possible and is usually 1 to 2 mm for experiments performed with this setup. The ejected electrons pass through a 1 mm diameter orifice of a skimmer, which separates the interaction

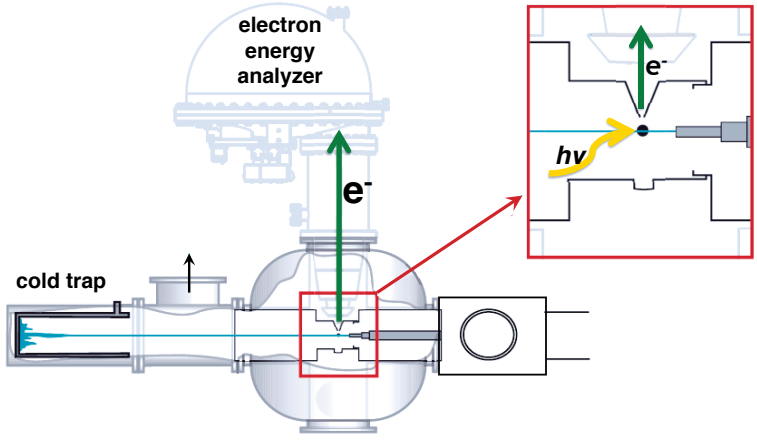

Figure 4.1. Schematic of the setup for XPS experiments on a liquid micro-jet at beamline I411 at MAX-lab, Lund University.

chamber from the differentially pumped analyzer chamber (operating at 10^{-5} to 10^{-6} mbar).

The liquid jet is created by a 20 μm thick glass nozzle, see figure 4.2. The sample is flowing through this nozzle usually with a speed of 20 to 40 m/s, depending on the backing pressure and inner-diameter of the nozzle. The temperature is held constant at 10° C until the jet enters vacuum. A liquid pump is used to push the sample solution through PEEK (Poly-Ether Ether Ketone) and stainless steel tubings with a constant flow of usually 0.5 ml/min. Under these conditions a free flowing, equilibrated liquid water beam in vacuum is obtained. After a few millimeters in vacuum the jet breaks into a train of droplets. Hence, the interaction with the monochromatic X-rays has to happen before this, between the first 2 to 4 mm downstream from the glass nozzle.

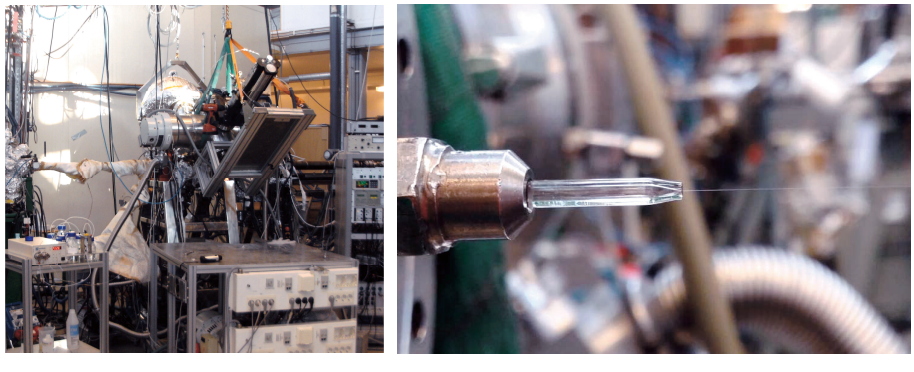

Figure 4.2. Photographs of the liquid jet setup at beamline I411 at MAX-lab in Lund (left) and a close-up on the glass nozzle with the thin micro-sized jet (right).

4.2 Equilibrium considerations

The local equilibrium of a surface of a liquid micro-jet is an eligible concern. XPS has to take place in vacuum, where due to the lower surrounding pressure, water will evaporate stronger than at standard conditions in the lab. Furthermore, the diffusion of species within the jet, to or from the surface, may not have come to a steady state at the time the liquid jet is probed by X-rays. Hence, results in terms of compound distribution as a function of distance from the surface may be interpreted incorrectly. Different groups have tried to examine the equilibrium conditions for XPS experiments on a liquid jet in vacuum. In the review article by M. Faubel and B. Winter [76], a discussion based on theoretical assumptions on water evaporation versus condensation is reported, concluding that the liquid micro-jet which traveled through vacuum for 1 mm is close to local thermodynamic equilibrium. M. Brown et al. [73] compared results from experiments on the same sample investigated at two different setups with different background pressures. XPS experiments at the advanced light source (ALS) in Berkley are performed at 3 mbar, while experiments at Bessy II in Berlin are performed at 10^{-5} mbar. They found no difference in the results, suggesting the lower pressure to be a less relevant parameter concerning a possibly disturbed equilibrium on the surface of a liquid jet. Diffusion times of solutes and water may differ strongly depending on the investigated compound, which affects the time a new surface is formed. While water and small ions can move around quickly in aqueous solutions, bigger, more hydrophobic molecules or ions can have longer diffusion times. For example, for water to move 100 nm it needs 2.3 μs [77], while butyric acid needs 5.5 μs [78]. In a recent study by Öhrwall et al. [79] performed at MAX-lab, the point of interaction after the liquid jet entered vacuum was varied. The investigated sample was a long-chained carboxylate salts, which probably has a longer diffusion time than many organic compounds studied in this thesis. The absence of spectral changes, within a time window of 40 to 300 μs after entering vacuum, implies that the system's equilibration time is either much shorter or much longer than the time scale accessed in the experiment. Further indication that the equilibration time is shorter than the tested time range is that in MD simulations typical equilibration times for surface phenomena are a few nanoseconds. The discussed results from different experimental setups, thermodynamic considerations and modeling indicate that the aqueous surface of the liquid jet has most probably sufficient time to form an equilibrated surface.

4.3 Raw data treatment and curve fitting

Prior to the deeper analysis of the recorded spectra, a normalization accounting for the number of recorded sweeps and the photon flux must be conducted. To account for the photon flux, the electron current inside the synchrotron ring is

used, as it was shown to be proportional to the delivered photons close to the last mirror before the interaction chamber. Spectra are energy-calibrated by shifting the $1b_1$ PE line of liquid water to 11.16 eV [14], see figure 3.1. Pure gas-phase spectra, which can be attained by lowering the jet out of the focus of the incoming X-ray beam and probing the gaseous phase above the liquid-jet, are energy calibrated against the gas-phase $1b_1$ PE line at 12.62 eV [13]. The PE lines of gas-phase species recorded simultaneously as the PE lines of liquid-phase species are often somewhat shifted towards lower BE energies as compared with the gas-phase binding energy of the pure gaseous species. This is believed to be explained by an attractive field near the liquid jet, that slows down ejected photoelectrons from gas-phase species close to the jet.

Curve fitting was done using the SPANCF fitting routine (*Spectrum Analysis by Curve Fitting*, E. Kukk, University of Turku, Finland) for IGOR Pro (WaveMetrics, Inc, Lake Oswego, OR, USA). Different line shapes can be chosen, where Voigt profiles, which are a convolution of a Lorentzian and a Gaussian lineshape, are mostly used to fit PE peaks from aqueous solutions. Also *post-collision-interaction* [80] (PCI)-profiles can be used to model PE peaks that show an asymmetry. Asymmetries can arise from vibrations within the molecule or variations in binding energy due to fluctuations in the solvation shell, and can usually not be fully characterized from results of these experiments. For a consistently agreeing analysis, spectra from binary sample solutions are often used as line shapes to constrain fitting parameters for the analysis of spectra of mixed solutions. Energy shifts, intensity ratios or peak widths of different spectra can be linked or fixed to specific values, to ensure consistent line profiles throughout the fit. Ratios of PE intensities can be calculated from results of a robust fit and further used for comparison with other experimental or modeled results.

4.4 Sample preparation and post-processing

High quality, commercially available chemicals and demineralized water (Millipore Direct-Q, 18.2 MΩ·cm) were used for preparing the sample solutions for all discussed experiments. Furthermore, prior to the XPS experiments, sample solutions were most often filtered (Whatman Puradisc FP30 syringe filters, 1.2 μm) to remove solid particles, which can severely disturb the flow at the nozzle. Sample solutions containing volatile compounds were usually not filtered to lower the risk for concentration changes. Information on the degree of dissociation are obtained from pH values, which can be converted to shares of the different forms in the bulk of the solution, see section 2.2.2. pH values of the samples were measured directly before or after XPS experiments at room temperature by using a portable pH meter (Thermo Scientific Orion 4-Star) equipped with an Orion ROSS Ultra electrode.

For pH dependent experiments of the same compounds, NaOH or HCl was used to adjust the pH of the solution. As mentioned in section 2.2, pK_a values found in literature are only valid for concentrations below 0.1 mol/dm^3. For higher concentrations a correction for ionic strength needs to be applied or the actual dissociation constant needs to be determined by standard acid-base titration. Besides titration, other techniques like NMR spectroscopy or density measurements can be useful to secure full information of bulk conditions, which is crucial when interpreting results of a surface-sensitive method.

As mentioned above, the PE intensity depends on the ionization cross-section and amount of the element of interest in the probed part of the solution, but also on the surface propensity. Highly surface-active molecules or ions can be studied even at very low concentrations. These species tend to accumulate at the aqueous interface, thus yielding high PE intensities. For example, for the case of C1s PE signal and no pronounced surface activity of the species of interest, a minimum concentration of about 0.1 mol/dm^3 still yields a reasonable signal. For surface enriched species this minimum concentration can be orders of magnitude lower. Nevertheless, to avoid charging effects, a minimum number of charged species are required for experiments on a liquid micro-jet. When probing for example deionized pure water, charging is observed through strongly shifting signals, as the sample is not electrically grounded via the experimental setup and the created electrons cannot be efficiently carried away. The addition of at least 0.025 mol/dm^3 of a neutral salt was found to be sufficient to enable charge transportation, i.e. electrical grounding of the sample solution.

4.5 What can be learned from PE spectra

In summary it can be said that the main advantages of XPS is the short escape depth of only a few nanometers, which enables probing of electrons from species in the surface region, and the chemical sensitivity. Though electrons are easily detected and counted, excellent vacuum is necessary for the experiments, which can be challenging in some cases. This technique is inherently surface sensitive, but bulk contributions are not negligible and the distinction of bulk and surface signal remains difficult to handle. In this section a short overview shall be given, emphasizing a few readily available interpretations and also common assumptions used during the analysis of results from XPS experiments.

4.5.1 PE intensity

The observed PE intensity at a given kinetic energy is proportional to the number and the photoionization cross section of the investigated species in the

probed volume, but exponentially attenuated with increasing depth, see equation 4.1. It is shown that the photoemission intensity I_{PE} can be expressed as being proportional to the integrated atomic density ρ (number per volume), exponentially attenuated by the electrons EAL with increasing depth [52].

$$I_{PE} = k \int \rho(z) exp(-z/EAL) dz \tag{4.1}$$

The constant k contains intrinsic material parameters, like photoionization cross-section [81], and parameters related to the experimental setup, like geometry of sample, photon flux and transmission function of the electron analyzer. These parameters are almost never known exactly, hence, absolute amounts cannot be quantified from PE spectra directly. However, qualitative information can be obtained from ratios of PE intensities of the same element under the assumption that variations of the photoionization cross-section, due to scattering of the outgoing photoelectron on neighboring atoms, is negligible for the studied species (section 3.4.1).

In surface-sensitive operation, i.e. when the kinetic energy of the photoelectrons is chosen to be between 50 to 150 eV, PE intensities reveal the *real* number distribution of species in the surface region, attenuated with increasing depth. Hence, information on the amount of the investigated species and its closeness to the surface can be gained, what is usually referred to as a species' surface propensity.

Comparing PE intensities within a sample

PE intensities of the same element recorded at the very same time, i.e. within the same spectrum can be easily related without much concern. PE intensities from different elements recorded at the same time require additionally exact knowledge about photoionization cross-sections of the different elements or even for different species to enable the derivation of quantified information. While these are usually not available, it is recommended to only compare PE signals from the same elements and possibly the same functional group within a compound, see section 3.4.1. That demands careful planning of the experiments, where many parameters should be evaluated. The addition of another compound to the solution that does not interact with the compound of interest, but possesses the same element, enables the comparison of their relative intensities. This is of course only possible if the PE lines of both compounds are sufficiently shifted in binding energy to allow correct fitting of the features. Attention has to be paid to possible chemical reaction between the co-dissolved species. Many studies have shown that the addition of another species to a solution can affect the solutes, even if they do not interact directly. It is therefore recommended to compare PE intensities between samples instead, which is explained in the followings.

Comparing PE intensities between different samples

Recorded PE intensities from different sample solutions can only be compared when spectra are acquired under stable conditions of the experimental setup and the light source, i.e. the probed volume has to be stable during data acquisition. In the experimental setup at beamline I411 at MAX-lab, the minimum acquisition time for one sample is roughly 1 hour, but can endure for several hours depending on the strength of the signal. During this time the intensity of the light source decreases gradually. Moreover, the alignment of the experimental setup can change over time due to vibrations and instabilities in the liquid jet, which results in an increasing or decreasing overall PE intensity. The decreasing X-ray intensity is accounted for as described earlier. If the alignment is not manually changed, samples are exchanged carefully and the synchrotron ring works smoothly, stable conditions for many hours can be achieved. To monitor the stability of the experimental conditions throughout a measurement series, the valence spectrum of a low concentration electrolyte solution, e.g. 0.05 mol/dm^3 NaCl, is usually used. The same solution is used to clean the sample injection system between the samples. In practice the $1b_1$ PE line of the liquid $1b_1$ state of this solution is compared. The variation in these signal intensities, which are usually of the order of 2 to 5 % for one series of experiments, needs to be included in the error bar estimation of the final analysis.

Ratios of PE intensities

PE intensity ratios yield mainly information on abundance and propensity of a species to the surface, as described above. If k in equation 4.1 can be considered to be the same for different species of interest, the ratio of their recorded PE intensities is equal to the ratio of the number densities in the probed volume, exponentially attenuated with increasing depth. Ratios of PE intensities of different species can thus be used to estimate the relative abundance of species in the probed volume. Ratios of the same element in one compound, but at different sites of it, can yield information on the orientation of the species with respect to the aqueous surface. As the EAL is usually not known exactly, mostly trends are discussed, while absolute numbers have to be treated with caution.

4.5.2 Estimation of surface concentrations

Species that yield a high PE signal usually exhibit a high surface propensity, i.e. they reside closer to the interface than species that are depleted in the surface region. Species with high surface propensity may accumulate at the aqueous surface, leading to an increased surface concentration. For species that show an increased surface propensity, results may allow the quantification of their surface-activity in terms of relative enrichment factors, which

relates their surface and bulk concentration. Resulting surface concentrations enable the direct comparison to other experimental or theoretical studies by e.g. estimating surface properties, such as surface tension. In the following two paragraphs, the two main approaches that are used in this thesis for the quantification of results from XPS experiments, in terms of concentration or relative enrichment, are described.

Surface concentration via EAL and surface width

To determine the surface concentration or the relative enrichment of a species versus another, a simple model is introduced, where it is assumed that the sample consists of a surface and a bulk layer with a step transition [82]. The total recorded PE signal of a species I_{tot} can then be described as the sum of the contributions from the surface I_s and the bulk I_b, where each contribution can be expressed by the respective concentration c and a sensitivity parameter n.

$$I_{tot} = k(n_s c_s + n_b c_b) \tag{4.2}$$

The sensitivity parameter accounts for the increased sensitivity of this method for the surface region. The constant k includes the cross-section and experimental alignment. The bulk contribution is estimated using a solute containing the same element but with negligible surface abundance, i.e. $c_s \approx 0$. The total recorded intensity of a surface-depleted compound $I_{tot,b}$ can then be described as:

$$I_{tot,b} = k n_b c_b. \tag{4.3}$$

With a conversion of equation 4.2 it can be shown that the relative concentrations in the surface and the bulk of the sample can be derived from ratios of the PE signal of the surface-enriched compound and the surface-depleted compound.

$$\frac{c_s}{c_b} = \frac{n_b}{n_s}\left(\frac{I_{tot}}{I_{tot,b}} - 1\right) \tag{4.4}$$

As surface-depleted species, formate ($HCOO^-$) is often used in studies where surface-active carbon-containing compounds, such as alcohols, alkylamines or carboxylic acids are studied [82]. Ammonium ions are suitable in comparison with nitrogen containing compounds, see supplementary information of paper IV. The estimation of the sensitivity factor $\frac{n_b}{n_s}$ is limited by the insufficient knowledge of the exact EAL values. In surface sensitive mode, the XPS signal is believed to be comprised of 50 $\pm$25% signal from the surface, which is a rather pessimistically estimated range. By assuming a physically reasonable EAL and the thickness of the surface layer of the investigated sample solution, it is possible to narrow this range. Using equation 4.1 and assuming the surface layer to extent between $0 \leq z \leq D$ and the bulk from $D \leq z \leq \infty$, the ratio of the bulk contribution I_b and the surface contribution I_s, $\frac{I_b}{I_s}$, can be related to

the sensitivity factor $\frac{n_b}{n_s}$, see paper I.

$$I_s \sim \int_0^D exp(-z/EAL)dz = EAL \cdot (1 - e^{-\frac{D}{EAL}}) \tag{4.5}$$

$$I_b \sim \int_D^\infty exp(-z/EAL)dz = EAL \cdot e^{-\frac{D}{EAL}} \tag{4.6}$$

The ratio of the bulk and the surface signal can then be expressed as:

$$\frac{I_b}{I_s} = \frac{e^{-\frac{D}{EAL}}}{1 - e^{-\frac{D}{EAL}}} \approx \frac{n_b}{n_s}. \tag{4.7}$$

The surface width D can be estimated from e.g. MD simulations or by using the compound's size.

Surface concentration via Langmuir-model

Surface concentrations of binary solutions can also be estimated from results of XPS experiments by analyzing the recorded PE intensities for increasing bulk concentrations. The Langmuir adsorption model describes adsorption of species to the surface by assuming no interaction between adsorbed species, equal adsorptions sites, where only one adsorbate can be accommodate. The theory was established by I. Langmuir in 1916 for the adsorption of gaseous molecules onto solid surfaces [23, 38] and is briefly introduced in section 2.3. Here, species with increased surface propensity are considered to be *adsorbed* to the surface from the bulk of the solution. The usage of a Langmuir model on results from XPS, were shown earlier by e.g. references 83, 84 and a similar procedure is applied to results presented in this thesis, see papers III and V.

The model describes the surface contribution I_s of the total recorded PE signal I_{tot} as a function of bulk mole fraction x_b, see equation 4.8. As the recorded PE signal contains bulk and surface contributions, I_s is given by the difference of I_{tot} and the bulk contribution I_b of the total recorded PE signal. I_b is often estimated by the signal recorded from a surface-depleted compound, as discussed in the previous paragraph.

$$I_s = \frac{I_{s,max} \cdot x_b}{x_b + (1 - x_b)e^{\frac{\Delta G^{ads}}{RT}}} \tag{4.8}$$

$I_{s,max}$ is the maximum PE signal expected for a completely saturated surface region, where I_s does not increase any further. The Gibbs free energy of adsorption ΔG^{ads} and $I_{s,max}$ are determined through the fitting of PE intensities with equation 4.8. The absolute temperature T is set to 283.15 K and the universal gas constant R = 8.31446 J/(K·mol). Subsequently, the portion p that is covered by solute species, also called the surface coverage Θ, can be derived from the ratio of I_s and $I_{s,max}$, see equation 4.9.

$$p = \Theta = \frac{I_s}{I_{s,max}} \tag{4.9}$$

$I_{s,max}$, which can be related to a molar concentration $c_{s,max}$, may be assumed to be a layer that only contains the solute. Hence, the pure compounds molar concentration can be used. Nevertheless, in some cases the surface of an aqueous solution, even though tightly packed with solute species, can contain a minimum amount of water incorporated into the structure. This implies that the maximum concentration is lower than the pure compound's concentration. Thus, depending on the solute and any additional available knowledge on the aqueous solution under investigation, final results and interpretations can vary and need to be adjusted. When agreed on a concentration $c_{s,max}$ that corresponds to $I_{s,max}$, the molar surface concentrations for any coverage can be obtained by multiplication.

A few assumptions are inherent within the Langmuir adsorption model, see section 2.3. Additionally, for the usage of XPS intensities as a measure of the surface coverage, a surface layer that is discrete from the bulk with a certain thickness needs to be assumed. Thus, the real surface concentrations might be over- or underestimated, depending on the studied case and should be, if possible, validated by comparison to literature values on e.g. coverage, molecular areas or results from MD simulations.

5. Summary and discussion of the results

A key issue of concern addressed in this thesis is the difference between the surface and the bulk behaviors of different solutes in aqueous solution. As discussed in chapter 2, solutes are assumed to be homogeneously distributed in the bulk of a solution, but the distribution of solutes in the surface region is often very different. Usually, surface-enriched and surface-depleted species are distinguished, as being intrinsic properties of solutes. Factors that determine the propensity of a certain species to reside close to the aqueous surface and the effect of the terminated hydrogen bonding network of water are lively discussed in the community and are also subject of this thesis.

A substantial feature of the XPS method, besides its element specificity and sensitivity to the chemical state, is its ability to sample information predominately from the surface region, when kinetic energies of photoelectrons between 50 to 150 eV are chosen. This combination makes this method ideal for the study of the structure and spatial distribution of species in the surface region, which is explained in detail in chapter 3. Here, results from surface-sensitive XPS experiments on a liquid jet, which were designed to elucidate the different chemical properties of the surface region of aqueous solutions on the molecular scale, are presented. Beyond the discussion on a species' inherent surface propensity and hydration structure, factors that lead to the deviating spatial distribution in the surface region in comparison with the bulk are systematically investigated.

In solutions with a single solute, the analysis and interpretation of a resulting enrichment or depletion of a species has been studied by many groups, [85, 86]. In nature, mixtures containing more than two solutes are common, but their investigation is experimentally rather challenging. It is difficult to disentangle intrinsic properties of the constituents and solute-solute interactions, such as complex formation, ion-pairing or effects of high ionic strength, from the resulting data. In this chapter, five selected publications are presented, which discuss examples that demonstrate the disparate behavior of various species at the aqueous surface and their implications for real systems. The publications cover results of aqueous solutions containing one or more solutes with ionic or molecular character. The discussion is arranged such as to start with results on single molecular species in water, where in particular relative enrichment, orientation and degree of coverage in the aqueous surface region is addressed. The enrichment of species is contrasted with examples on ionic species, which tend to stay in the bulk of a solution. In the second part, results from model solutions reflecting more real aqueous systems are summarized.

In these studies, see papers IV and V, results of solutions containing more than one solute are presented, where interactions between dissolved compounds are discussed.

5.1 Surface behavior of single solutes

Organic molecules are often of amphiphilic nature, as they consist of a hydrophobic part, such as an alkyl-chain, and a hydrophilic part, e.g. carboxylic acid or hydroxyl group. Hydrogen bonds are accepted or donated by these polar functional groups, while the interaction of water with hydrophobic alkyl-chains are rather unfavorable as they may disrupt the natural hydrogen bonding network of water. Even small organic compounds with little hydrophobic parts are known to decrease surface tension of a solution as compared to pure water, which is explained by a certain surface-propensity of the compound. Compounds with a strong surface-propensity, i.e. surface-active compounds, can accumulate at the aqueous surface, which results in an altered spatial distribution of solutes close to the air-water interface. As it is impossible to form hydrogen bonds with vacuum, this interface can be viewed as a hydrophobic surface, where hydrophobic interactions are enhanced. Depending on their molecular structure, the orientation of the species at the surface can be distinct and result in specific adsorption behaviors, mainly driven by the minimization of interactions between hydrophobic parts and water. Additional contributions from interactions between different hydrophobic functional groups, such as van der Waals interactions between methylene groups of alkyl-chains, may amplify the surface propensities of certain compounds. In papers I, II and III, results of surface-sensitive experiments on organic molecules in aqueous solutions, such as a dicarboxylic acid and various alcohol isomers, are presented. In particular succinic acid and alcohols with four to six carbon atoms were investigated to explore the segregation of these species to the interfacial region as well as changes in the surface structure with different bulk concentrations. Furthermore, different approaches were used to quantify surface concentrations of these compounds. In the following subsections, these results are outlined and contrasted with results on ionic species in solutions, which were found to be effectively depleted in the surface region.

The studies on short-chained (< 8 carbons) organic species are mainly motivated by atmospheric chemistry, as these oxidized compounds constitute a large fraction of aerosol particles [87, 88]. These organic molecules, which are oxidation products of volatile compounds in the atmosphere, have low vapor pressure and can therefore contribute substantially to aerosol particle loading. Especially the connection between surface tension reduction and surface-to-bulk partitioning of such molecules in aqueous environments are of high interest in the atmospheric community [50, 89].

Succinic acid was chosen, because it is moderately soluble in water and its physico-chemical properties have been investigated both experimentally and theoretically in the past years, see e.g. references 90–92. This enables the comparisons of XPS results to macroscopic properties of this acid. The molecule consists of two carboxylic acid groups, which are attached to each side of an alkyl-chain, and it can be deprotonated in two steps with pK_a values of 3.83 and 5.13, see supplementary information of paper I. Thus, at pH values > 8, a majority of the organic species in solution are doubly charged.

Alkyl-alcohols are oxygenated, short-chained species, which are composed of a number of methyl, methylene groups and a hydroxyl group. With the same composition, these molecules can have different structures, which can alter their interactions on the molecular scale and affect even macroscopic properties, such as vapor pressure or surface tension [93, 94].

5.1.1 Surface propensity of solutes

In figure 5.1 the C1s PE spectra of aqueous succinic acid, denoted as $SuccH_2$ ($HOOC(CH_2)_2COOH$), and aqueous succinate ions, denoted as $Succ^{2-}$ ($^{-}OOC(CH_2)_2COO^{-}$), are shown together. The spectra were recorded in quick succession using a photon energy of 360 eV. The PE intensities are given in arbitrary units, but the relative intensities can be compared directly. Two PE lines are observed for each form of succinic acid, originating from the chemically equivalent carbon atoms of this symmetric molecule, which are chemically shifted due to their different direct molecular environment. The binding energy of the carboxylic acid groups and the alkyl-chain is 294.4 eV and 290.7 eV, respectively. Both lines are shifted towards lower binding energies for the fully deprotonated species, which are found at 293.2 eV and 289.8 eV, respectively. The shift to lower binding energies originates from the increased shielding of the carbon nucleus due to the excess negative charge. These results reflect the inherent chemical sensitivity directly, which facilitates the direct observation of the protonation state close to the air-water interface, as it was exploited in other studies on similar compounds [79, 82].

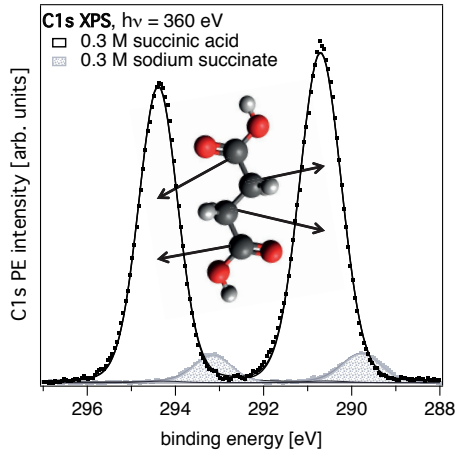

Figure 5.1. C1s PE spectra of 0.3 M aqueous succinic acid and succinate ions. Note, the relative intensity scale of the different traces is the same.

The signal intensity of succinic acid is significantly higher in comparison with the intensity recorded from succinate ions at the same bulk concentration, which is given in mol/dm^3 (denoted as M) here. The ratio of the signal at this particular bulk concentration is found to be roughly 12 and allows to conclude that the fully protonated form is strongly enriched in the surface region as compared with the fully deprotonated form. The difference in recorded PE signal is possibly composed of a bigger propensity of the acid to reside close to the air-water interface and a greater overall abundance in the surface region. To disentangle these two contributions of the PE signal and enable the estimation of surface concentrations, a variety of approaches can be applied, each based on a few assumptions, see section 4.5.2. The most conservative estimate to derive a range of relative surface concentrations from ratios of PE signals of the same element is based on the estimate that the recorded PE signal is comprised of 50 $\pm$ 25 % of the surface. This yields sensitivity factors $\frac{n_s}{n_b}$ between 1/3 and 3. Applying this approach, see also section 4.5.2, to results on succinic acid and succinate ions, a so-called surface enrichment factor, which relates the molar surface to bulk concentration, can be estimated. For a 0.3 M succinic acid solution enrichment factors between 4 and 33 are obtained. Thus, succinic acid does not only have a higher propensity to reside close to the air-water interface in comparison with succinate ions, but it also is more abundant in the surface region.

A similar comparison between mono-carboxylic acids and their deprotonated conjugates can be conducted. For this purpose C1s PE spectra were recorded from solutions of 0.1 M butyric acid ($CH_3(CH_2)_2COOH$), 0.1 M sodium butyrate ($CH_3(CH_2)_2COO^-$) and 0.5 M sodium formate ($HCOO^-$) in

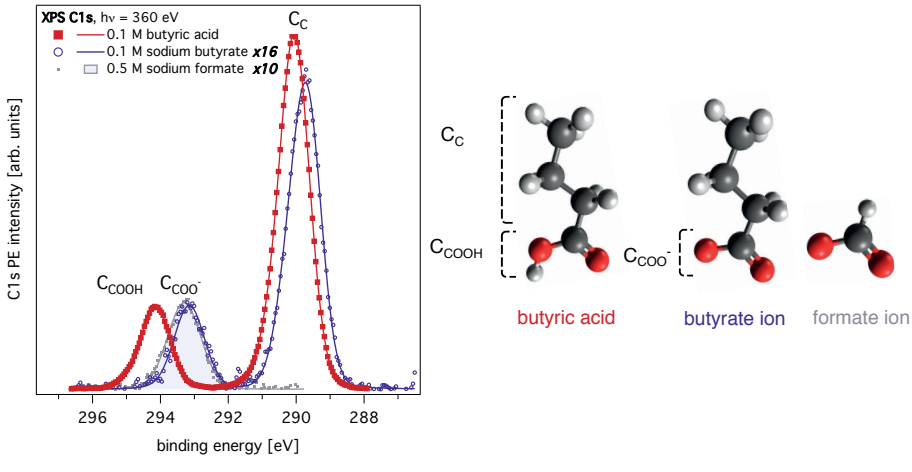

Figure 5.2. C1s PE spectra of 0.1 M aqueous butyric acid, sodium butyrate and 0.5 M sodium formate are shown together with schematics of these chemical compounds. Note, the spectra of the ionic forms are scaled by the indicated factors.

quick-succession under stable conditions of the experimental setup and the X-ray source. The resulting spectra are shown in figure 5.2, where the intensities of butyrate and formate are scaled as indicated. The alkyl-chains (C_C) of these compounds are found at electron binding energies of > 291 eV. The carbon atom that is in direct neighborhood to the oxygen atoms, i.e. the carbon atom of the carboxylic acid group (C_{COOH}) and the carboxylate group (C_{COO^-}), are well-separated and found at binding energies < 292 eV. From the strongly deviating C1s signals, it can be already speculated that formate is depleted in the surface region, while butyric acid and butyrate ions are enriched in the interfacial region to different extents. Note, the higher bulk concentration of formate ions has to be taken into account for the comparison with other organic compounds.

From the total PE signals of these compounds, the ratio between each of them and formate was derived, taking into account the difference in bulk concentration. Together with the above applied conservative estimate, the compounds' relative surface enrichment factors were determined. This enables the ordering of the compounds with similar number of carbon atoms but different functional groups according to their surface-activity in comparison with formate ions. Butyrate ions yield the lowest range of surface enrichment factors with 1 to 5, while butyric acid yields values from 18 to 165. Note, the enrichment factors given are strongly concentration dependent and the direct comparison with succinic acid values is not equitable here. Resulting enrichment factors from concentration-dependent studies are subject of the subsequent section.

The origin of the different degree of surface-propensity is found in the interplay between these compounds and the solvent water molecules, which in turn strive to minimize unfavorable interactions with the hydrophobic alkyl-chains. The competition between these processes and the interplay of water and solutes at the air-water interface and in the bulk of solutions will be discussed in more detail later. Here, it can be concluded that different organic compounds possess increased propensities to reside close to the aqueous surface, which is accompanied by a strongly increased abundance of the studied compounds in the surface region.

5.1.2 Concentration dependent investigation: surface enrichment and depletion

To elucidate the behavior of oxygenated organic compounds at the aqueous surface in more detail, to quantify surface concentrations and to deepen the understanding of surface coverage, the discussion of concentration-dependent studies of organic compounds proceeds in this section. In particular the results presented in papers I, II and III are compared, which report results on aqueous

succinic acid, primary alcohols and some of their secondary or tertiary isomers. Furthermore, results on ionic solutes, in particular succinate ions and ammonium ions, and their behavior in the surface region in contrast to the behavior of the molecular species, are discussed.

Succinic acid

In paper I results on a systematic study of succinic acid and succinate ions as a function of bulk concentration is presented. C1s spectra of pure succinic acid and sodium succinate solutions at increasing concentrations up to close to the bulk solubility limit of succinic acid, which is at 0.543 M at 20° C, were measured and the recorded intensities as a function of bulk concentration are shown in figure 5.3.

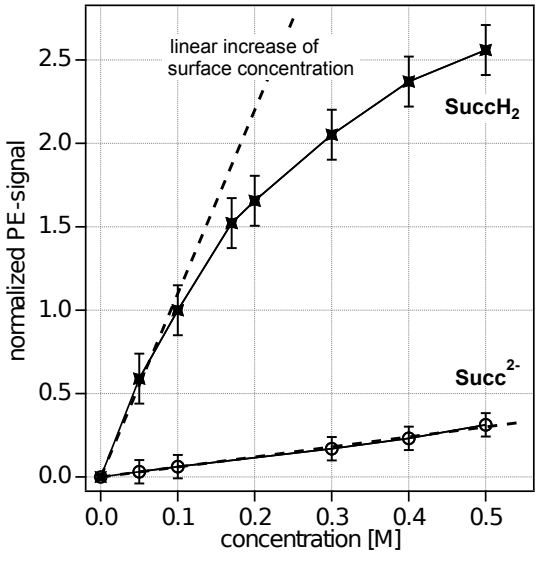

Figure 5.3. Recorded C1s PE intensities of aqueous succinic acid and sodium succinate solutions at different concentrations. Paper I - Reproduced by permission of the PCCP Owner Societies.

The curve is strongly bent for the acid, while the PE signal of succinate ions follows a straight line with an overall much lower value. The PE signal originating from succinic acid molecules does not increase equally strong at higher bulk concentrations, which leads to the conclusion that the diacid molecules start to saturate the surface region. The PE signal of succinate ions on the other hand increases linearly with bulk concentration. The proportional increase of the PE signal together with results from MD simulations is explained by a strong depletion of the divalent ions from the aqueous surface region. A similar behavior has been found for ammonium ions (NH_4^+) in ammonium chloride (NH_4Cl) solutions, which show linearly increasing N1s PE signal as a function of bulk concentration, see supplementary information of paper IV. This behavior is expected for small ionic species, as the Debye-Hückel and Gibbs adsorption theory suggest [95, 96]. The latter relates a net surface excess concentration to a reduction in surface tension, and a net depletion of a solute to an increase in surface tension with respect to the surface tension of pure water. For the studied ions, the surface tension shows an increasing trend, thus confirming the suggested surface depletion [97, 98]. Furthermore, results from MD simulations of the studied ions show strongly decreasing density profiles upon approaching the interfa-

cial region, see papers I and IV. The assumption that the recorded PE signal originates from species in the surface-near bulk of the solution is thus justified.

Alkyl-alcohols at the aqueous interface

Aqueous solutions of alkyl-alcohols and their corresponding positional isomers have been investigated, where both alkyl-chain length and bulk concentrations were varied over a wide range from very dilute solutions up to close to the solubility limit. Isomers in general have the same molecular formula, $C_xH_{2x+1}OH$, but different connectivity, i.e. the hydroxyl group is attached at different positions. For the primary alcohols, the hydroxyl group is attached to the terminal carbon, while for secondary alcohols the hydroxyl-group is situated in the middle of the alkyl-chain, see figure 5.4.

Alkyl-alcohols containing four to six carbon atoms in total were chosen for detailed studies, see figure 5.4, and results are reported in papers II and III. Here, the main findings are discussed. In figure 5.5 the recorded C1s PE intensities of aqueous solutions of 1-pentanol and 3-pentanol are shown versus the bulk concentrations. It can be seen that the recorded PE intensities increase with increasing bulk concentration for both isomers, where the C1s PE intensity of 1-pentanol is higher than the C1s PE intensity of 3-pentanol for all concentrations. For the highest investigated bulk concentration, the signal does not increase any further. As both curves show this saturating behavior, it can be concluded that both isomers have an increased propensity to reside close to the air-water interface, which results in accumulation of these molecules in the surface region.

Results of additional experiments on aqueous 1-butanol, *tert*-butanol, 1-hexanol and 3-hexanol, presented in paper III, show similar trends. Solutions of primary alcohols yield a higher PE signal than their corresponding positional isomer. This indicates that the linear alcohols reside closer to the air-water interface and are overall more abundant in the interfacial region than their branched isomers, which cannot be packed as effectively as linear alcohols in all-trans configuration. The concentration-dependent C1s PE signals

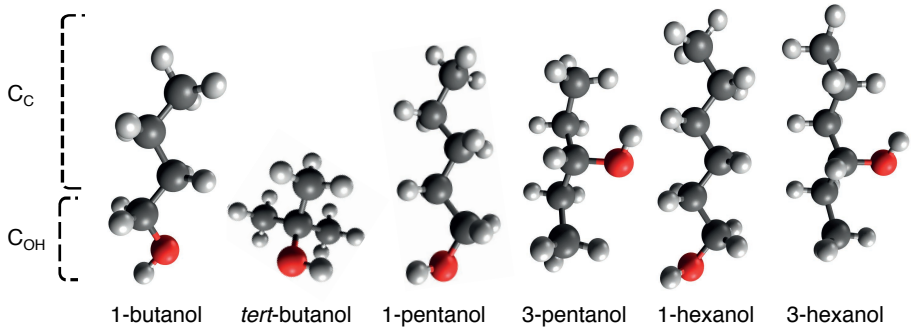

Figure 5.4. Schematics of the studied alkyl-alcohol isomers.

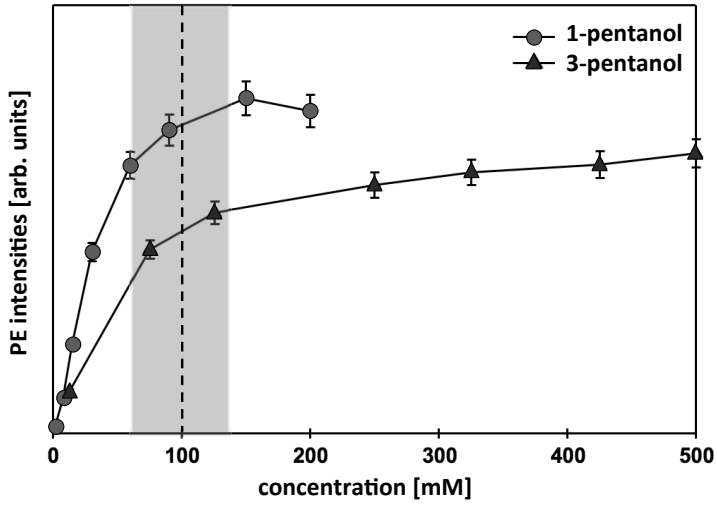

Figure 5.5. Recorded C1s PE intensities of aqueous 1- and 3-pentanol solutions at different concentrations. Adapted from paper II with permission of the PCCP Owner Societies.

from all different alcohols show a reduced increment at bulk concentrations > 200 mM for butanol, > 100 mM for pentanol and > 40 mM for hexanol, dividing the curves into two regions, as indicated in figure 5.5 for 1- and 3-pentanol. Above these concentrations, the PE signal only increases slightly, as the immediate surface is saturated with alcohol molecules and more and more alcohol molecules must reside in the sub-surface and bulk region. C1s PE intensities from dilute solutions increase strongly with concentration but mostly proportional to the increasing bulk concentration, which describes the gradually filling of the surface sites by alcohol molecules. At the above listed concentrations, a certain surface coverage is reached, which can be described as a mono-layer like structure because it features effective packing of the amphiphilic solutes.

Comparing the recorded PE intensities for all investigated alcohol solutions with the compounds' bulk solubility limits, it is found that the lower solubility correlates with a higher PE signal [16]. *tert*-butanol is freely miscible with water, while the other studied alcohols have a solubility limit. Nevertheless, also *tert*-butanol accumulates in the surface region, leading to the typical saturation of the C1s signal at high bulk concentrations, like the solubility-limited long-chained alcohols.

5.1.3 Orientation of organic compounds and surface structure

Besides the investigation of the full range of C1s PE intensities of succinic acid and the alkyl-alcohols, XPS enables also the detailed study of the behavior of

the functional groups itself. Due to the chemical shift of the core-level photoelectrons, differences in their atomic-scale chemical and physical environment can be distinguished. For the compounds discussed in this chapter, the C1s PE spectra contain mostly two distinct lines corresponding to the methyl and methylene groups, C_C (at BE < 290 eV) and the oxygenated functional groups, C_{OH} or C_{COOH} (at BE > 291 eV). The ratio of the peak areas of C_C and C_{OH} or C_{COOH} were evaluated to gain information about the relative orientation of the investigated species. The average PE ratio of molecules randomly oriented in the probed volume should be close to the stoichiometric ratio of the species, e.g. 4 for pentanol. Nevertheless, a better measure is the ratio obtained from gas-phase PE spectra, due to possible differences in the cross-section of the different carbon atoms, see section 3.4.1. As molecules in the gaseous phase are randomly oriented, a deviation between the ratio of the dissolved compound and the ratio from the gas-phase, indicates a preferential orientation of the species at the aqueous surface. A gas-phase spectrum of succinic acid cannot be attained from XPS experiments above an aqueous solution, because the diacid is not very volatile and does thus not evaporate sufficiently to detect it above a liquid jet. The PE intensity ratio of the methylene groups and the carboxylic acid groups of aqueous succinic acid was determined to be 1.17 for all studied concentrations. This value is slightly higher than the stoichiometric ratio of 1, suggesting that the methylene groups are closer to the air-water interface compared to the carboxylic acid groups. The fact that this ratio is unchanged over a wide range of concentrations and roughly the same also for the deprotonated conjugate, it can be anticipate that the orientation towards the aqueous surface is not changing. Reports on aqueous succinic acid studied by other experimental and modeling approaches give the conclusion that succinic acid orients mostly with the carboxylic acid groups on the same side of the molecule's methylene backbone, while the latter is oriented parallel to the aqueous surface plane [99, 100], which is in line the study presented in paper I.

For the different alcohol molecules, spectra of the gaseous phase were obtained and ratios were found to be close to the stoichiometric values. Ratios were determined for all studied aqueous alcohol molecules and found to be dependent on the concentration of the solution. In figure 5.6, see also paper III, the ratios for all studied alcohols are plotted as a function of concentration. It can be seen that the ratio increases in the first region up to approximately the concentration, where the increment of the recorded PE intensities changes, and decreases subsequently. This trend has been observed for all investigated alcohols, but with stronger extent for longer linear alcohols, e.g. 1-hexanol. The ratios of the butanol isomers vary only little over the studied concentration range.

The low ratio determined from results of dilute solutions, indicates that the alcohol molecules at the surface are oriented with their alkyl-chain parallel to the aqueous surface plane, which was confirmed by MD simulations, see

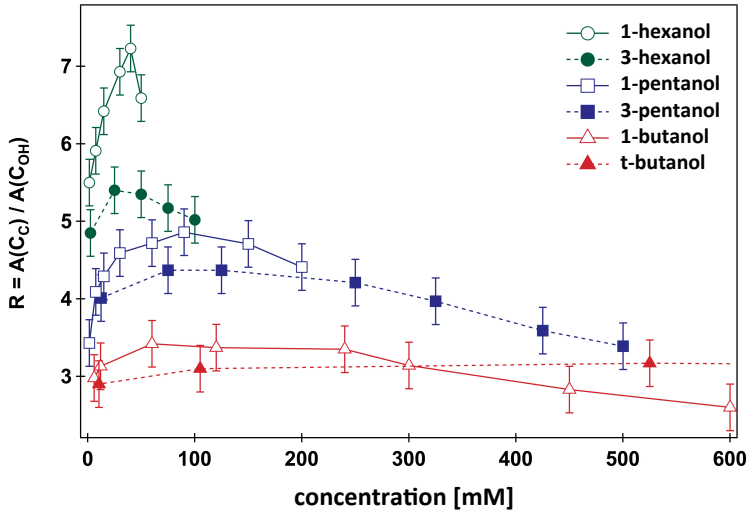

Figure 5.6. C1s PE intensities ratios of the studied alcohol isomers in aqueous solutions at different concentrations.

paper II. Thus, all carbon atoms contribute equally to the recorded PE signal, see figure 5.7 left side. When the concentration is increased, gradually more alcohol molecules adsorb at the aqueous surface, which leads to interactions between the molecules. The increasing ratio suggests that the alcohol molecules choose to point their hydroxyl groups towards the bulk solution, while the alkyl-chains turn towards the vacuum side as depicted in figure 5.7 right side. As the PE signal is exponentially attenuated along its path, the described orientation thus leads to the enhancement of the PE signal of the alkyl-chains and the dampening of the signal from the hydroxyl carbon. The primary alcohols are in total longer in all-trans configuration than their positional isomers, which explains the more pronounced change in the PE signal ratio when the molecules gradually "stand up". The same reason explains also the stronger deviation of the ratio from the stoichiometric one for the alcohols with longer alkyl-chain. At even higher concentrations the ratio for all isomers is decreasing again due to the increasing contribution of the surface-near-bulk region, which is increasingly populated with molecules in random orientation.

Core-level PE lines from aqueous solutions have usually rather fixed binding energies, which is probably due to the dominating water-solute interactions in the direct vicinity of the monitored core-levels. Hence, a deviation implies a change in the chemical and physical local molecular environment. Interestingly, results of the concentration-dependent study on alcohol isomers with different alkyl-chain length show that the C1s binding energy, especially of the carbon atoms of the alkyl-chain, changes significantly over the studied concentration range. As presented in paper II, the effect is pronounced for 1-pentanol and considerably weaker for 3-pentanol. To quantify this effect, the

binding energy difference ΔBE of the hydroxyl carbon and the alkyl-chains were determined for each concentration. Generally, ΔBE decreases with increasing concentration and it is found that both pentanol isomers have the same relative binding energy at the concentration, where the monolayer-like structure is obtained, i.e. around 100 mM. At low concentration, ΔBE is very high for 1-pentanol with 1.54 eV and rapidly decreasing with increasing concentration. In contrast to this, ΔBE of 3-pentanol is 1.36 eV in the region < 100 mM and constant within the error bars. For higher bulk concentrations ΔBE decreases to a minimum of 1.28 eV for 1-pentanol and 1.17 eV for 3-pentanol. The relative binding energies are found to arise mainly from a shift of the C1s PE line of the alkyl-chains to higher binding energies, whereas the binding energy of the hydroxyl carbon stays constant within experimental sensitivity. These findings indicate a gradual desolvation of the methyl and methylene groups and a simultaneous increase of van der Waals interaction between the alcohol molecules that accumulate in the interfacial region. The net effect is a reduced screening of the C1s electron, which results in the increased binding energy as compared with the same molecule only interacting with surrounding water molecules instead. 3-pentanol shows a similar effect, but not as pronounced, indicating that the molecular-scale environment of the

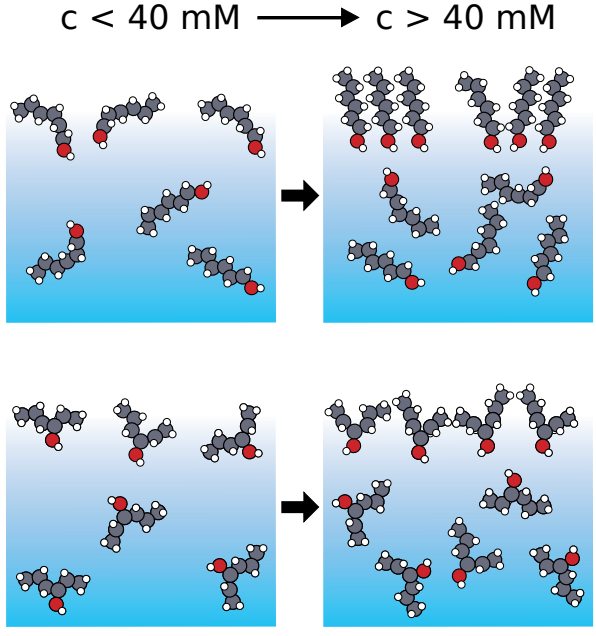

Figure 5.7. Schematic of 1- and 3-hexanol at low and high concentration. The left side shows the surface adsorbed molecules, which lie within the surface plane. The right side shows the tightly packed surface region, where the alkyl chains point towards the vacuum side, while the hydroxyl group point towards the aqueous phase.

alkyl-chains is only slightly changing with concentration. The short alkyl-chains point towards the vapor phase, where they are partially desolvated at increased bulk concentrations. Similar trends have been observed also for the shorter and longer alcohol isomers, with stronger changes for hexanol and less strong changes for butanol, see supplementary information of paper III.

5.1.4 Hydration motifs of solutes at the surface compared to bulk

After reviewing the results from XPS experiments on aqueous solutions of different oxygenated organic compounds, see paper I, II and III, the link of the reported results to hydration motifs and driving forces behind the outlined observations are summarized in the following. In the beginning of this chapter surface propensities of different solutes are compared based on their relative PE intensities. The origin of the different relative surface propensities of the studied compounds is found in the interplay between solute and water molecules, i.e. their strength of hydration. Furthermore, a solute or water molecule that resides at the air-water interface lacks neighboring molecules in one direction compared to a molecule in the bulk. Thus, solute and water molecules strive to minimize the system's energy by occupying surface or bulk sites in such a way that the species which causes the highest increase in energy when residing close to the aqueous surface, resides in the bulk. On the other hand, species which can be partially dehydrated without causing a gain in energy for the aqueous system, can reside at the air-water interface. In this regard it becomes clear that the geometry of the solutes and their hydration shells play an important role.

Amphiphilic species, e.g. 1-pentanol, butyric acid or butyrate ions possess hydrophilic and hydrophobic parts. For the examples mentioned here, the alkyl-chain constitutes the hydrophobic part, which interacts more or less unfavorably with water depending on its size. Water forms a *void* around these parts of the molecules to minimize these interactions and maximize the preferred water-water interactions [36]. The hydrophilic functional groups of the investigated species, i.e. the hydroxyl group and the carboxylic acid or carboxylate group, form strong hydrogen bonds with water. This explains why the studied compounds reside preferentially closer to the aqueous surface than e.g. formate ions. Due to their amphiphilic structure, these solutes can reside close to the air-water interface, where interactions between the alkyl-chain and water are reduced to a minimum.

The different relative surface propensities of the studied solutes can also be explained in terms of relative strength of hydration. As shown in section 5.1.1, butyric acid yields a stronger PE signal than butyrate ions, even though both compounds have a similar structure and equally many carbon atoms in the alkyl-chain. Only their functional groups discerns the two compounds, as butyrate ions lack a proton and are thus negatively charged in comparison with

the electrically neutral butyric acid. The -COO^--group is stronger hydrated compared with the -COOH-group due to its charge, which allows the protonated butyric acid to reside closer to the aqueous surface. It has been shown by theoretical approaches, that a carboxylic acid group forms on average 2.5 hydrogen bonds, while the deprotonated form (-COO^-) forms 6 [36], which supports the suggested interpretation.

Water disfavors the interaction with alkyl-chains of these molecules, as they interrupt the strong hydrogen bonding network of water molecules in the aqueous bulk. From the study of alcohol molecules with different numbers of alkyl-carbon atoms, it can be concluded that the alkyl-chains are partially dehydrated at the air-water interface at increased concentrations, see figure 5.7. With the alkyl-chains pointing towards the vapor phase, the interactions with water are minimized and a portion of the solutes are stabilized in the interfacial region without increasing the net energy of the aqueous system, as the effect of increased unfavorable water interactions would yield. A side-benefit is that less water molecules need to reside at the direct surface, as these sites are partially filled with amphiphiles. Also non-linear, secondary alcohol compounds and dicarboxylic acids, see papers I, II, III and reference 101, are found to have their methyl and methylene groups on average closer to the aqueous surface than their oxygenated functional groups. The disfavor of bulk water molecules to surround the alkyl-chains in combination with the benefit of reducing the amount of water molecules in the immediate air-water interface, where neighboring hydrogen bond acceptors or donators are missing completely, enforces this behavior. The difference between the non-linear and linear solutes is that the latter can lower their energy additionally by van der Waals interactions with neighboring alkyl-chains in close packing. When sufficiently many molecules reside in the interfacial region, the additional lateral interactions can stabilize the linear alcohols effectively. The interactions with neighboring alkyl-chains lead to the described effective packing of the primary alcohols in the surface region yielding low molecular areas as compared to the branched alcohols, with roughly 40 $Å^2$ and 60 to 70 $Å^2$, respectively.

Succinic acid, which possesses two carboxylic acid groups that form hydrogen bonds with water, is overall more strongly hydrated than the studied alkyl-alcohols. As the hydrophilic functional groups are located on each side of the molecule, a possible dehydration of the two methylene groups in the center of the molecule requires the whole molecule to be located close to the aqueous surface. Nevertheless, it is concluded in papers I and V that a partial dehydration of the center part of succinic acid is possible at high concentrations, where the surface region is tightly packed with molecules, but the effect is probably less strong compared to the primary alcohols.

Water molecules have in general stronger interactions with ionic species. Thus, embedding ions into the hydrogen bonding network of bulk water is favorable. A few results on ionic compounds, reported in this thesis, have been discussed already, in particular formate ions, ammonium ions and the divalent

succinate ions. All of these have been found to avoid residing in close vicinity to the air-water interface. Water forms tightly bound hydration shells around these ionic species, effectively screening the charge of the ions. As the amount of available water molecules for hydration is decreasing close to the aqueous surface, ionic species are, if possible, situated in the bulk of the solution to maintain full hydration in all three dimensions. A few exception have been found, where a special geometry of the species, asymmetric hydration patterns or high polarizability reduce the requirements for hydrating water molecules, see discussion on paper IV and e.g. reference 4 for details.

5.1.5 Surface enrichment factors and interfacial concentrations

Absolute amounts of a certain species are generally not directly available from PE spectra, as the exact EAL for a given kinetic energy of the photoelectrons ejected from an aqueous sample solution is not known at present. However, the quantification of the above discussed relative abundance of certain compounds compared to others would enable the direct comparison with results from other approaches or could be used as input for models of aqueous systems and is thus worth striving for. Specifically the partitioning of solutes, which are known to be abundant in atmospheric droplets, was investigated. A future-aim in this context is a parameterization for, e.g. the relative enrichment as a function of length and branching of the alkyl-chain, functional group and bulk concentration, which allows to use these results for e.g. modeling of properties of aqueous systems. The term enrichment is used in this context to describe the ratio of surface and bulk concentration, which is a measure of the relative partitioning of the solutes between the surface and the bulk region in a solution. Note, enrichment factors can relate mole fractions, molal or molar concentrations, which are different quantities. The various approaches that have been used in this thesis to quantify the concentration of a compound in the surface region are described in section 4.5.2. In papers I, III and V, these were applied to results of aqueous solutions of succinic acid and alkyl-alcohols. For all approaches, the recorded total PE intensity has to be compared to the PE signal of a compound that is assumed to be strongly depleted in the surface region. For the succinic acid project, the recorded C1s PE signal of succinate ions was used to mimic the bulk contribution to the recorded succinic acid C1s intensity. For the different alcohol isomers the C1s PE signal of formate ions was utilized instead.

The previously applied conservative sensitivity factors (see section 5.1.1) can be refined using a physically reasonable range of EAL together with a surface thickness taken from e.g. results of MD simulations, see paper I. This approach was applied to estimate the sensitivity factor, see equation 4.7, for succinic acid solutions. The resulting range of enrichment factors and surface concentrations were further used to model surface tension, where the major

remaining uncertainty origins from the lack of the exact knowledge of the EAL as described above. The comparison with experimentally obtained surface tension values is satisfactory for the different approaches, as discussed in paper I. Even though, the choice of surface tension model, activity model and range of EALs, affects the results somewhat. Using the more advanced surface tension model introduced by Sprow and Prausnitz [39, 40], and later used by Li et al [41], together with the UNIFAC activity model [31, 102], enrichment factors based on molal concentrations in the range of 19 to 24 reproduces the experimentally obtained surface tension values best. This means, given that the determined surface thickness is reasonable, an EAL of roughly 7 Å needs to be assumed.

The curves showing the recorded PE signal as a function of bulk concentration, figures 5.3 and 5.5, resemble the shape of Langmuir adsorption isotherms that can be used to describe the portion of the surface area that is covered by adsorbed molecules as a function of bulk concentration of the solute. Based on the Langmuir adsorption theory, a model is proposed that can be used to determine the surface contribution of the recorded PE signal as a function of bulk concentration [83, 84], which is described in details in section 4.5.2. The results on pure succinic acid in aqueous solutions, which are reported in paper I, were revisited using this approach, see paper V. Equation 4.8 matches the data nicely and a Gibbs free energy of adsorption of -12.8 kJ/mol is determined for aqueous succinic acid, see figure 5.8 a). The second fit parameter, $I_{s,max}$, corresponds to the PE signal that is observed for a fully saturated surface volume. The portion of the maximum value gives the degree of saturation in percentage at any concentration. Close to the bulk solubility limit, roughly 70 % of $I_{s,max}$ is reached. In order to derive surface concentrations using the PE signal portions of the various studied bulk concentrations, the molar concentration corresponding to $I_{s,max}$ needed to be estimated. For this concentration, the pure compound's concentration could be assumed or a surface concentration where a minimum amount of water molecules is incorporated into the structure, for example like the first hydration shell, which has to be decided depending on the solute of interest and additional available knowledge. For the succinic acid project, the maximum possible concentration was estimated by choosing a value that reproduces experimental surface tension data, using the same surface tension model as described above. With 8 M corresponding to $I_{s,max}$, surface tension values were reproduced very well, see figure 5.8 b). Surface concentrations c^s as a function of bulk concentration were calculated using equation 4.8 and are shown on the right axis in figure 5.8 a).

Results on a concentration-dependent XPS study of alkyl-alcohols, which show Langmuir-like behavior, are presented in paper III. The obtained PE intensities as a function of concentration were fitted using the same model as described in section 4.5.2. Resulting fits agree reasonably well with the data points, where stronger deviations are observed for longer linear alcohols, while the asymmetric alcohols are overall better matched. Despite these dis-

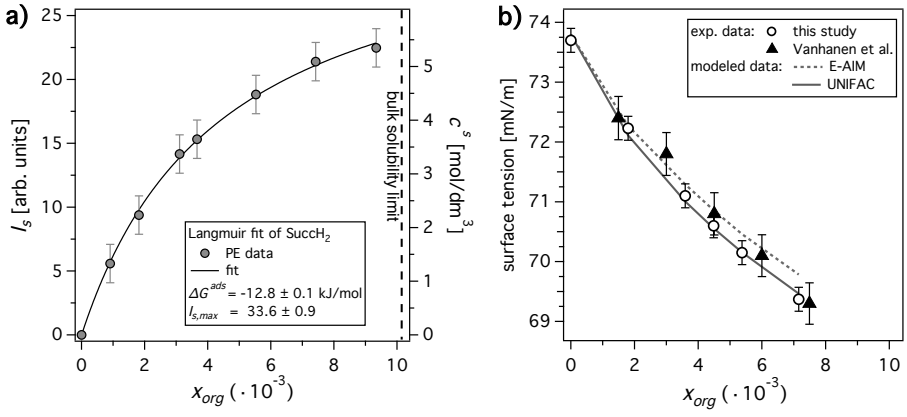

Figure 5.8. a) Surface PE intensities I_s of aqueous succinic acid as a function of bulk mole fractions x_{org} with Langmuir Fit, see equation 4.8. The right axis shows corresponding molar surface concentrations c^s. b) Experimental (Vanhanen et al. [36] and paper V) and modeled surface tension as a function of x_{org} aqueous $SuccH_2$ for two different surface tension models.

crepancies, Gibbs free energy of adsorption ΔG^{ads} are found to scale linearly with the number of alkyl-carbon atoms, with about -2 kJ/mol per methylene group.

In comparison with succinic acid, all studied alcohols have a more negative free energy of adsorption, which means that these solutes have an overall higher surface propensity. 1-butanol, which also has four carbon atoms, has an adsorption energy of -15.3 kJ/mol, which means the aqueous system gains 2.4 kJ/mol more energy by stabilizing butanol instead of succinic acid in the interfacial region. Perrine et al. [84], who studied aqueous solutions of thiocyanate ions, determined the ion's Gibbs free energy of adsorption to be -6 kJ/mol, which is roughly half the value found for succinic acid. This is reasonable as the thiocyanate ion is charged and more strongly hydrated. The energy gain due to adsorption of a compound to the surface region can be viewed as a measure of the compound's relative surface propensity and enrichment. An important parameter, affecting the surface propensity and enrichment of a compound, is their hydration structure and strength in the surface and bulk regions, respectively. Hence, solute-water interactions determine the partitioning of compounds in aqueous systems. In connection to the previous section on hydration structure and strength of the discussed solutes, it can be concluded that succinic acid, which is composed of two carboxylic acid and two methylene groups, is stronger hydrated than e.g. 1-butanol, but weaker than a small ion, such as thiocyanate, which leads to their relative enhancement in the interfacial region and the difference in ΔG^{ads} values.

Molar surface concentrations of the studied alcohols are found to be roughly 100 times higher compared with bulk concentrations. This is 5 to 10 times

stronger than enrichment factors determined for succinic acid and can be explained by the different hydration strength of these compounds. The studied alcohols only contain one hydroxyl group that favorably interacts with water, while a dicarboxylic acid has two strongly hydrated carboxylic acid groups. Additionally the longer alkyl-chains, which can stabilize each other by van der Waals interactions, when densely packed, can contribute to the net energy balance. The enrichment factors given in paper III show a maximum at low concentrations, which is most pronounced for the hexanol isomers. It is also found that the surface concentrations of the linear alcohols are overall higher than their branched isomers. Due to their two shorter alkyl-chains, the molecule requires more space and cannot be packed as efficiently as the linear alcohols in all-trans conformation [94]. The branched alcohols can thus not be dehydrated at the aqueous surface to the same extent as the linear alcohols, which is why their surface concentrations are lower than the surface concentrations found for linear alcohols. This is similar for succinic acid molecules, which are likely to be only partially dehydrated at the aqueous surface.

Another interesting fact is, that the higher surface concentration of the studied alcohols correlates roughly with their bulk solubility, where the lower bulk solubility results in a higher concentration in the surface region, see paper II. As mentioned above, the proposed Langmuir model for results of surface-sensitive XPS experiments differ increasingly more, the longer the linear alcohol molecules are. For 1-hexanol the slope of the curve seems steeper for low bulk concentrations, which leads to a S-shaped curve [38]. Hence, an adsorption mechanism involving two steps could be considered, where the molecules are adsorbed individually in the first step. For higher concentrations the surface region is increasingly filled with alcohol molecules, which start to interact directly via their hydrophobic alkyl-chains. This leads to the second step where the adsorption increases strongly.

5.2 Mixtures of solutes in solution

After the detailed discussion of the behavior of various molecules at the aqueous surface in the previous section, results from solutions containing more than one solute are outlined in the following. Results presented in paper IV deal with mixed solutions of two inorganic salts, while results presented in paper V address mixed solutions of an organic acid with inorganic salts.

There is a variety of ions that play an important role in different aspects of life and the molecular-scale origin on chemical and biological implications are often not clear. In living systems mixtures containing more than one solute are common, where the different ions are important for essential functions, such as maintaining the membrane-potential between cells or support of vital functions concerning, e.g. the neural system. Many important reactions in biochemical systems are driven by hydrophobic interactions but take place in

an aqueous environment, e.g. peptide-membrane interactions or protein folding [103]. Guanidinium ions ($[C(NH_2)_3]^+$, denoted as Gdm^+) are frequently used protein denaturants, which unravel the protein's three-dimensional structure that minimizes its exposed surface. Ammonium and guanidinium ions are functional groups in a few of the most common amino acids, e.g. arginine and lysine. In proteins, these amino acids often have similar functions, though interchanging them modulates key properties of the protein. Hence, from biochemical point of view, a detailed characterization of the behavior of these compounds in solution and at aqueous surfaces is of great interest. The following subsection focuses on results of mixed aqueous solutions containing guanidinium and ammonium chloride, where, besides their intrinsic properties, also interactions such as ion-ion interaction upon co-dissolution are elucidated.

In the second part, results on mixed solutions of succinic acid and inorganic salts are outlined and discussed. Results on pure succinic acid solutions were already presented in paper I, but in this part the study is extended to mixed solutions containing additionally ammonium sulfate ($(NH_4)_2SO_4$) or sodium chloride (NaCl). Such mixed solutions are commonly found in atmospheric aerosol particles, where succinic acid, as being an oxidation product of biogenic volatile compounds, represents a typical organic molecule with moderate surface-activity and solubility in the aqueous phase. Sodium chloride comes often into the atmosphere from sea spray over oceans while ammonium sulfate is typically emitted by anthropogenic sources over rural sites. Hence, these mixtures can be viewed as model particle contents representing atmospheric aerosol particles with different origins. From atmospheric science point of view, interactions between inorganic ions and molecules and their relative partitioning in particles are of major concern and their molecular-scale origin is largely unexplored. Studies investigating macroscopic properties, such as evaporation, uptake or surface tension showed that many physicochemical properties cannot be modeled using results of the two pure ingredients and may rather be explained by non-linear interactions between the compounds, see e.g. references 104, 105. Results on mixed solutions are summarized and discussed in section 5.2.2.

5.2.1 Mixed solutions containing guanidinium and ammonium ions

The behavior of ions at the aqueous surface is shortly touched upon before, when discussing succinate and ammonium ions, which are studied as a function of bulk concentration. It was concluded that small ions are generally expected to be strongly depleted in the surface region [95, 96]. Nevertheless, this classic picture has been severely shaken by theoretical and experimental studies during the last decade, suggesting an enhanced abundance of big po-

larizable halide ions at the water-vapor interface [1, 4, 106]. Though most studies agree on this general behavior, the exact origin and the extent of the enhancement are still intensely debated.

Guanidinium and ammonium ions were investigated in aqueous solutions, see paper IV. The main interest here is to understand the behavior of the cations in mixed solutions, where the common anion is chloride. In XPS experiments, the two cations can easily be distinguished by monitoring their respective N1s lines, which are sufficiently separated with binding energies of 405.2 eV and 406.7 eV for guandinium and ammonium ions, respectively. This enables the study of the relative surface composition of equimolar ammonium and guanidinium chloride solutions, i.e. the same concentration of each salt, with increasing bulk concentration within the same spectrum. From N1s spectra, ratios of the peak areas were obtained, where it should be noted that Gdm^+ contains three equivalent nitrogen atoms, arranged around a carbon atom, while NH_4^+ only contains one nitrogen atom. Thus, ratios of the N1s PE intensities were calculated and subsequently divided by three. Furthermore, corresponding aqueous solutions were simulated using MD simulations. Applying equation 4.1 and a range of reasonable EAL values, resulting simulated density profiles were used to compute PE intensity ratios and the results were combined with the experimentally obtained ratios, see figure 5.9. It can be seen that the ratios of Gdm^+ and NH_4^+ from surface-sensitive XPS experiments increase non-linearly with increasing total concentration. This indicates that Gdm^+ has a stronger propensity to reside close to the aqueous surface than NH_4^+.

From the study of mixed solutions containing Gdm^+, NH_4^+ and chloride ions, only relative information of the behavior of the compounds in the interfacial region is gained. Intrinsic properties and ion-ion interactions may contribute positively or negatively to the net outcome. Therefore, a series of experiments with a constant alignment of the XPS setup and the photon source was conducted, where PE intensities of solutions containing only one salt were compared among themselves and with mixed solutions. Additional to the cations, which were again monitored via their respective N1s PE lines, the anion abundance in the surface-near region was recorded via the Cl2p PE lines. Results show a decreased NH_4^+ signal and an increased Gdm^+ signal in the N1s spectra of mixed solutions compared with the spectra of the pure solutions. This indicates that Gdm^+ is pushed closer to the surface in the presence of ammonium chloride, while NH_4^+ is stronger depleted in the aqueous surface when co-dissolved with GdmCl. In combination, these results can be interpreted as a partial replacement of ammonium ions by guanidinium ions in mixtures.

For further support of this interpretation, the anion's PE lines of the same solutions were monitored and it was found that guanidinium-containing solutions show higher PE intensities than the pure ammonium chloride solution. As the excess of positive charges in the surface region due to an increased

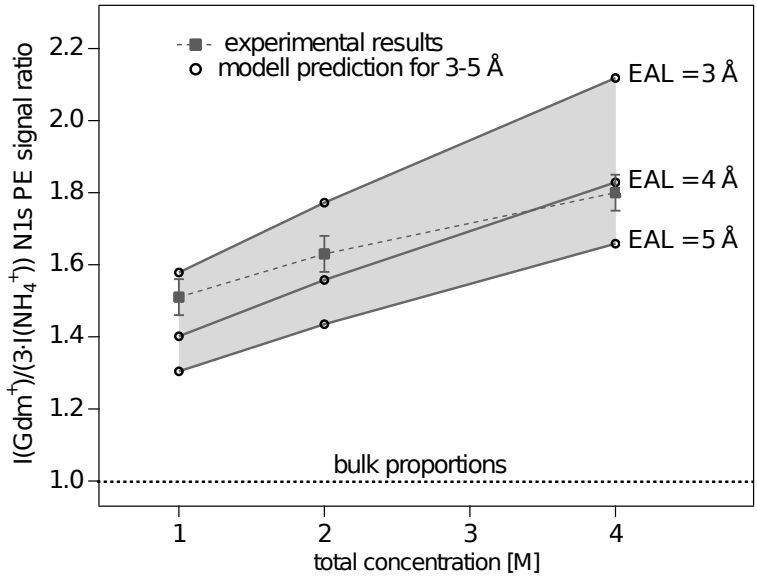

Figure 5.9. Ratios of N1s PE signals, $I(Gdm^+)/(3 \cdot I(NH_4^+))$, as a function of total concentration in equimolar solutions of GdmCl and NH_4Cl. Results from surface-sensitive XPS experiments are displayed together with results from MD simulations for a range of EALs of 3 to 5 Å. Reprinted with permission from paper IV. Copyright 2014 American Chemical Society.

amount of guanidnium ions, must be matched by an excess of counterions to ensure local charge-neutrality, the comparison of Cl2p intensities support the increased propensity of guanidnium ions to reside close to the surface. A closer look on the comparison of the pure GdmCl solution and the solution where half of the Gdm^+ is exchanged by NH_4^+, reveal no significant change in the chloride abundance in the surface-near region. This allows to conclude that guanidnium is indeed pushed towards the aqueous surface by ammonium ions.

It can be concluded that in mixed solutions, beyond the replacement of NH_4^+ by Gdm^+ in the surface-near region, Gdm^+ is also pushed closer to the interface by NH_4^+ at elevated concentrations in equimolar mixed solutions. This effect is often referred to as salting-out. Molecular-scale considerations on hydration structure and origin of the ions' surface behavior are discussed in the end of this section together with the results on mixed solutions containing organic molecules and inorganic ions, which are presented in the following.

5.2.2 Succinic acid in aqueous electrolyte solutions

While it is clear from the previous section that multi-component solutions are more difficult to fully understand, such studies are crucial for the understand-

ing of real aqueous systems. Direct or indirect interactions between solutes and their effect on their relative surface behaviors in mixed solutions containing molecular and ionic species are discussed below.

In section 5.1 many aspects of the surface behavior of succinic acid in pure solutions are discussed. Below, results on a study where mixed solutions of succinic acid and either NaCl or $(NH_4)_2SO_4$ were probed, are presented (paper V). Note, concentrations are given in [mol/kg H_2O], which is denoted as m, or mole fractions x in this study. An intermediately strong succinic acid concentration of 0.25 m was chosen. At this concentration, which corresponds to a mole fraction of $x_{org} = 0.00459$, the surface is not saturated, see figures 5.3 and 5.8 a). Leaving the organic acid concentration constant in this series of experiments, different amounts of NaCl or $(NH_4)_2SO_4$ were added to the solution, creating more or less strong electrolyte solutions. To investigate the effect of either of the inorganic salts on the surface propensity and distribution of succinic acid in the surface region, C1s PE intensities of the mixed solutions were recorded. In figure 5.10 a) the ratio of the recorded C1s intensities from mixed solutions and a pure succinic acid solution containing the same amount of succinic acid are plotted as a function of inorganic salt concentration. It can be directly seen that the signal from the organic acid is increasing with increasing amounts of either $(NH_4)_2SO_4$ or NaCl. As it is known from the study on pure succinic acid solutions, this dicarboxylic acid is enriched in the surface region. Hence, this further increase of the PE signal indicates that the addition of inorganic salts increases the succinic acid concentration

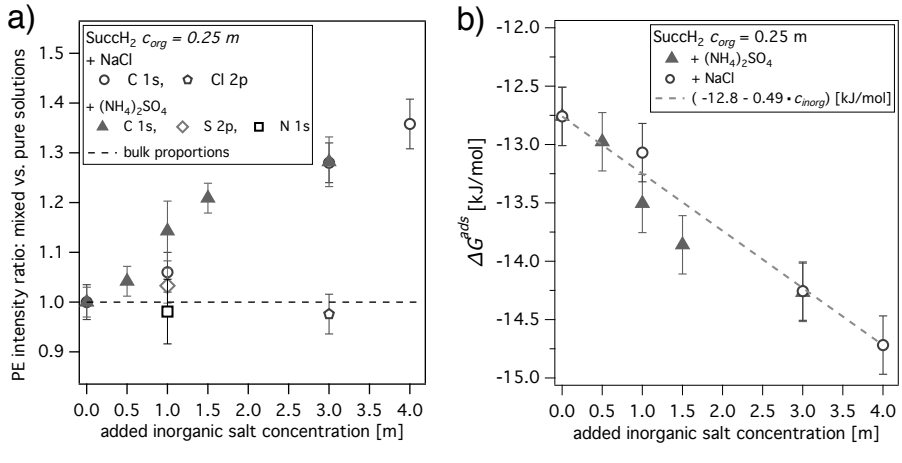

Figure 5.10. a) C1s, Cl2p, N1s and S2p PE intensity ratios of XPS results from mixed solutions containing succinic acid and various amounts of NaCl or $(NH_4)_2SO_4$ and corresponding pure solutions. The dashed line indicates the bulk proportions. b) ΔG^{ads} derived using the Langmuir model (equation 4.8) under the assumption that the surface is only populated by succinic acid and the bulk contains both inorganic ions and succinic acid.

in the surface region even further. This is also known as salting-out effect of the acid by inorganic ions in solution, similar to the reported results on aqueous guanidnium and ammonium ions in paper IV. Furthermore, the effect of the co-dissolved organic acid on the surface behavior of the inorganic ions was studied by monitoring the N1s PE intensities of ammonium ions, the S2p intensities of sulfate ions and the Cl2p intensities of chloride ions in mixed solutions and pure electrolyte solutions. Resulting ratios of these core-level intensities are added to figure 5.10 a) and are found to be unaffected by the addition of succnic acid. It can be stated that the spatial distribution of ions in the probed volume is not affected upon addition of succinic acid, which is expected for strongly hydrated ions that mainly reside in the bulk of the solution.

To quantify the salting-out effect of inorganic ions on succinic acid molecules, the previously introduced Langmuir-model was utilized with an additional assumption. Pure succinic acid solutions were well described by this model and resulting surface coverages were further used to derive surface concentrations of the acid in pure solutions via the maximum coverage $I_{s,max}$ and its free energy of adsorption ΔG^{ads}, which was found to be -12.8 kJ/mol, see figure 5.8 a). Assuming that this maximum coverage cannot be exceeded by this particular diacid, because it corresponds to a tightly packed layer only containing succinic acid and water, equation 4.8 can be used to derive a ΔG^{ads} for the electrolyte solutions as well. Using the increased surface PE signal of the mixed solutions and rearranging equation 4.8, ΔG^{ads} as a function of electrolyte concentration were computed and results are shown in figure 5.10 b). The observed negatively increasing trend supports the interpretation of increased amounts of succinic acid at the aqueous surface with increasing inorganic salt concentration. The derived ΔG^{ads} values can be viewed as a measure of the net energy gain of the aqueous system, accomplished by pushing the organic acid to the interface. Furthermore, the "new" ΔG^{ads} for each inorganic salt concentration enables the derivation of adsorption isotherms for different amounts of succinic acid. Together with the adsorption isotherm for pure succinic acid solutions, this allowed the estimation of the surface coverage for any combination of succinic acid with NaCl or $(NH_4)_2SO_4$, see figure 3a in paper V. Possible usage of this parameterization is discussed in section 5.3 in connection with atmospheric implications. This model with the extended assumptions was used to estimate surface concentrations of succinic acid and surface tension data were modeled using the same approach as described in section 5.1.5. The successful comparison with measured surface tension values, see figure 3b in paper V, confirms that the introduced assumptions are reasonable for the studied mixed solutions.

5.2.3 Effect of competition for hydrating water molecules

The results and interpretation of the studies presented in papers IV and V allow to draw a few more conclusions on the origin of the observed surface behaviors. In both studies, a strong deviation from bulk proportions was observed at the air-water interface, which is stronger at elevated concentrations in comparison with low concentrations. When less water is available for hydrating the ions and molecules in solution, the species that interacts less strongly with water is pushed closer towards the aqueous surface.

In case of the guanidinium-ammonium solutions, the hydration enthalpies of these ions were compared and found that NH_4^+ has a lower value than Gdm^+, -329 kJ/mol and -502 kJ/mol, respectively [107, 108]. Per individual amine group, ammonium is thus stronger hydrated compared to guanidinium. Nevertheless, hydrogen bonds between guanidinium and water are on average stronger, because it forms two hydrogen bonds per amine group compared to four per ammonium ion, see figure 5.11.

Furthermore, the size and geometry of the ions are rather different. Guanidinium is planar and considerably bigger than the symmetric ammonium ion. The guanidinium ion donates hydrogen bonds to water almost exclusively parallel to its molecular plane, as depicted in figure 5.11 and exhibits only very weakly interactions between water and its quasi-aromatic π-system [109]. It is also known that guanidinium ions do not disturb the strong hydrogen-bonding structure of water considerably [110]. It is capable to pair with like-charge ions or other molecules due to its flat "faces" [111, 112]. Having this in mind, the obtained results suggest that guanidinium can approach the aqueous surface because of its unique hydration shell. A detailed MD simulation study proposed a partial dehydration of the flat faces of guanidinium, that allows

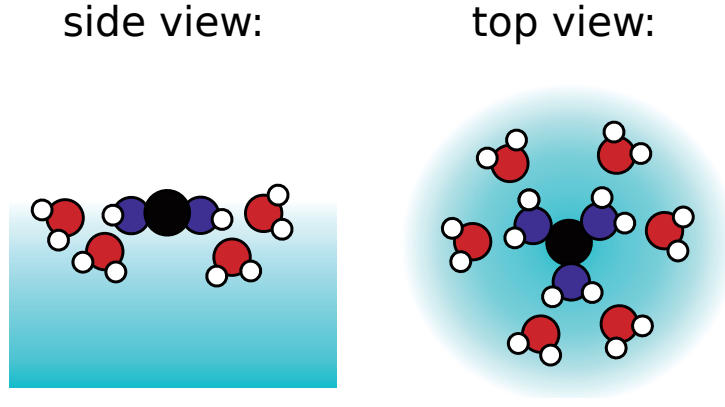

Figure 5.11. Schematic of the hydration of a Gdm^+ ion, which can reside close to the aqueous surface being oriented parallel to it, as it forms hydrogen bonds with water only within the plane.

the cation to approach the air-water interface closely when aligned parallel to it [113]. The unique property of this flat ion to integrate in a two-dimensional water hydrogen network, is the reason for the relative excess of guanidinium at the aqueous surface. As it donates strong hydrogen bonds only within the plane, the hydration at the less favorable surface-near sites is possible. Ammonium ions, which interact strongly with water and require hydrating water molecules in three dimensions, reside in the bulk of the solution, as it is concluded in section 5.1.2.

In case of the mixed solutions containing a molecular and ionic species, the conclusions are similar, although a few fundamental differences should be discussed. Succinic acid is considerably weaker hydrated in comparison with the inorganic ions in the mixed solution. The weak hydration of succinic acid is discussed above and shall only be repeated quickly here. The two carboxylic acid groups form weak hydrogen bonds with water, while the two methylene groups, which interact unfavorably with water, constitute a counterbalance reducing the strength of interactions of this molecule with water. The inorganic ions, namely ammonium, sulfate, sodium and chloride are overall strongly hydrated and known to be depleted in the surface region. Thus, in a mixed solution, water in the bulk of the solution favors the hydration of the inorganic ions and succinic acid is increasingly segregated to the surface. At high electrolyte concentrations, the amount of available water is strongly reduced leading to a competition for hydrating water molecules. Succinic acid molecules, which are possibly partially dehydrated at the air-water interface, are preferentially incorporated into the surface-water structure, as they do not require hydration in all dimensions.

5.3 Implications for atmospheric aerosol particles

Succinic acid, monocarboxylic acids and alkyl-alcohols are, among others, known to be abundant in atmospheric aerosols [87, 114]. Due to their low volatility, these compounds can contribute to atmospheric aerosol loading, as it is unlikely that these compounds will leave the particular phase via evaporation. A few consequences for the properties of aerosol particles, which can be deduced from the increased surface concentrations, see papers III and V, are pointed out in this section.

The concentrations of the studied compounds in the surface region of pure aqueous solutions are extremely increased in comparison with their bulk concentrations. That means, that more of the molecular species can be accommodated in a particle with a certain water content. As small particles have a high surface-to-volume ratio, the smaller the particles is, the larger the relative organic content can become. To illustrate this effect and show its strong particle size-dependence, a bulk-like particle and a 2-phase particle are compared. A bulk-like particle, which is depicted in figure 5.12 a), contains homogeneously

distributed solutes. A 2-phase particle on the other hand, consists of a surface and a bulk phase with the corresponding different concentrations, as depicted in figure 5.12 b).

Considering a saturated particle containing one organic compound and water, the number of moles of the organic compound and water was estimated. For this estimation, a surface thickness and ideal mixing of all constituents needed to be assumed. A saturated particle means, that the bulk volume is loaded according to the bulk solubility limit of the compound and the surface, which has a thickness d_s, contains the corresponding organic surface concentration determined from XPS results, see papers III and V. In figure 5.13 the total dissolved organic ratio is shown as a function of the wet particle diameter for 3-pentanol, succinic acid and 1-hexanol. The total dissolved organic ratio is the number of moles of dissolved organic compound in a 2-phase particle divided by the number of moles of organic compound in a bulk-like particle of the same size. A surface width of 4 Å was assumed for succinic acid and 3-pentanol, and 6.5 Å for 1-hexanol, see papers I and III for details. It can be seen that the dissolved organic content increases strongly with decreasing wet particle diameter. This effect is more dominant for the stronger enriched compounds. 1-hexanol reaches twice the total particle content at about 425 nm, while 3-pentanol at about 35 nm and succinic acid at about 25 nm. The results demonstrate that due to the increased amount of dissolved organic compound in the surface region compared with the bulk volume, smaller particles can contain overall a multiple of the expected value of a bulk-like particle. This may help to explain why small particles stay liquid and internally mixed, as compared to bigger particles with the same relative content, which are found to be phase-separated [51, 115, 116]. For a given size, if the organic loading is not exceeding the corresponding value, the particle thus can be considered to be in the liquid aqueous phase as opposed to partially solid.

In Köhler theory, particle activation, i.e. cloud condensation nuclei (CCN) activation, is described using equation 2.15, where supersaturation is expressed

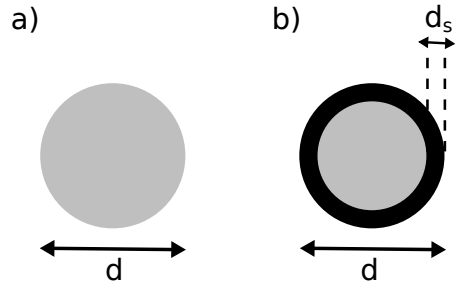

Figure 5.12. a) Bulk-like particle, which contains homogeneously distributed solutes. b) 2-phase particle, which contains a surface phase of thickness d_s. Both particles have the same total diameter (d).

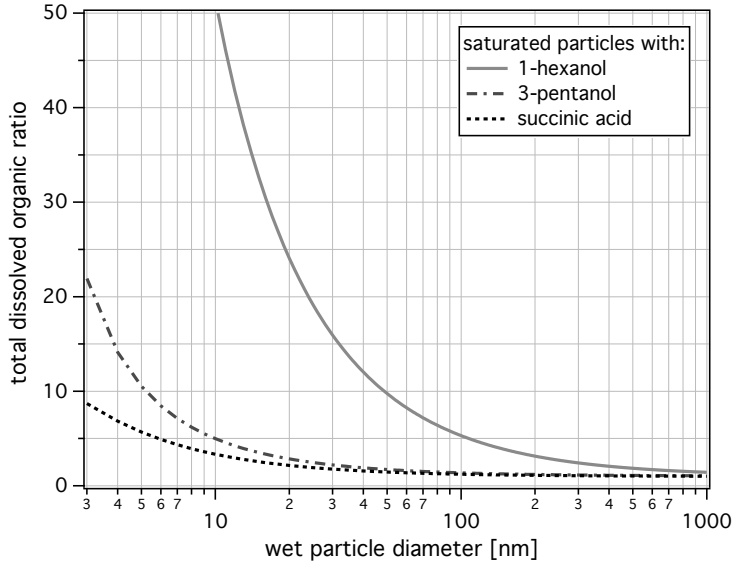

Figure 5.13. Total dissolved organic ratio of saturated particle containing 1-hexanol, 3-pentanol or succinic acid are shown as a function of wet particle diameter.

as a combination of the Kelvin effect and the Raoult effect, see section 2.3.1. Surface-active compounds accumulate at the surface and reduce surface tension, which enters the Köhler equation via the Kelvin term. Partitioning of surface-active compounds enters the Köhler equation also in the Raoult term, as it can be viewed as a depletion from the bulk and hence affects the bulk water activity. This is often neglected in equilibrium growth estimations. Sorjamaa et al. [50] showed that the full account for surfactant partitioning in both the Kelvin and the Raoult term lead to a decrease in cloud droplet activation, when compared with only taking into account surface tension lowering. The impact on partitioning on the two terms in the Köhler theory counteract each other partly, which indicates the importance of getting the best estimate for both: surface enrichment and changes in the surface tension [117]. These effects are size-dependent, as the presented results in this thesis suggest. Taking into account surface effects implies that the total amount of dissolved organic compound is enhanced in small particles.

In paper V, results from XPS experiments on mixed solutions containing succinic acid and NaCl or $(NH_4)_2SO_4$ are presented. It is shown that the presence of inorganic ions push succinic acid towards the surface leading to an increased surface concentration. Assuming a particle that contains a certain relative amount of succinic acid, inorganic salt and water in the bulk volume, the total amount of organic in the particle was calculated as a function of wet particle diameter. The inorganic ions were assumed to be only abundant in the bulk, as it is discussed in paper V. Figure 5.14 a) shows the total dissolved

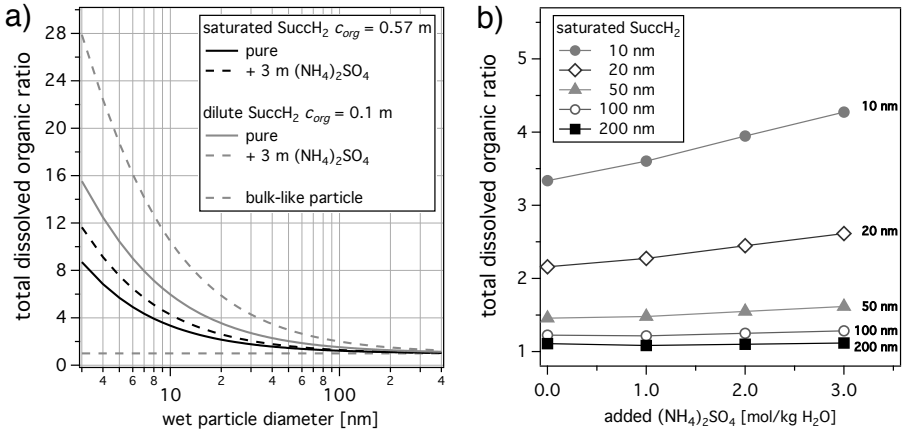

Figure 5.14. a) Total dissolved organic ratio as a function of wet particle diameter with and without additional $(NH_4)_2SO_4$. Two cases are shown: the saturated and a dilute succinic acid concentration. b) Total dissolved organic ratio for a saturated succinic acid concentration as a function of added $(NH_4)_2SO_4$ for different wet particle diameters.

organic ratio for different particle diameters. Two cases are compared, a dilute and a saturated succinic acid concentration, i.e. the maximum amount of the organic acid in the bulk and at the surface. The pure cases are compared to the loading of a particle containing additional 3 m $(NH_4)_2SO_4$ in the bulk volume. It can be seen that the electrolyte in the bulk volume of a particle affects the total organic loading more strongly, for the low than for the high succinic acid concentration. This leads to the conclusion that the *salting-out effect* is stronger for the dilute organic concentration than for the saturated concentration, which is attributed to the relative coverage of the surface. The surface is only covered to a small degree for the low organic concentration and the addition of electrolytes can enhance the succinic acid surface concentration substantially. The surface of a saturated particle on the other hand is already covered to a large degree and the additional strongly hydrated ions in the bulk volume cannot increase the amount of organic acid at the surface equally strong. Nevertheless, the inorganic salts enhance the total succinic acid concentration in the particle in both cases. Similar findings based on results of a surface tension study on comparable aqueous systems, have been reported [118]. The enhanced surface concentration implies that particles containing both inorganic salt and organic acid are in the liquid aqueous phase, already for higher particle diameters as compared with particles that only contain the organic acid.

To illustrate the effect of the inorganic salt content in the bulk of the particle on the organic loading of the particle, the total dissolved organic ratio is plotted as a function of added $(NH_4)_2SO_4$, see figure 5.14 b). Here, a particle containing the saturated succinic acid concentration is considered only. The

different lines correspond to different wet particle diameters. It can be seen that smaller particles are more strongly affected by the additional dissolved inorganic ions than bigger particles. A 10-nm-particle can contain a multiple of organic acid together with a considerable amount of inorganic salt and can still be considered to be in the liquid aqueous phase as compared with e.g. a tenfold bigger particle.

CCN activation is strongly affected by the presence of inorganic salts. Already small amounts of sodium chloride are shown to increase the tendency to activate strongly [119]. The reason may lie in an increased water uptake when inorganic salts are present. Connected to this should be mentioned that liquid particles activate more readily than dry ones, because the barrier caused by the solid core of undissolved material is absent [119, 120]. Hence, the phase state matters strongly for CCN activation and as shown in figures 5.13 and 5.14. The phase of a particle is strongly size dependent for a given composition and should therefore be considered, when modeling particle activation processes and related properties.

6. Conclusion and outlook

In this thesis aqueous solutions of environmentally relevant compounds are investigated, e.g. organic molecules and inorganic salts known to be abundant in atmospheric aerosols, and ionic species, which are important functional groups in amino acids, using X-ray photoelectron spectroscopy. The key features of this particular spectroscopic method enables the study of the aqueous surface, in particular due to the surface-sensitivity and element specificity, which facilitate the monitoring of the chemical state of a species at the same time. From trends of relative PE intensities conclusions on the structure and composition of the air-water interface are evaluated. In the first part, i.a. the orientation of alcohol isomers with different alkyl-chain length as a function of concentration is discussed. At high concentrations, the alcohol molecules point with their aliphatic chain towards the vapor phase while the hydroxyl group stays in the liquid phase, where sufficient hydration is enabled. This orientation implies that a part of the alkyl-chain is dehydrated, which is confirmed by the observed changes in the relative chemical shift ΔBE. The relative PE intensities of the same core-level in different compounds helped to understand the relative propensities and enrichments of different molecules. It is found that succinic acid is more abundant in the aqueous surface than its deprotonated form. Through the comparison between butyric acid, butyrate and formate ions, it is found that non-charged species can approach the aqueous surface much closer than their charged conjugates. Investigating the behavior of alkyl-alcohols as a function of bulk concentration showed that these molecules indeed start to saturate the air-water interface as they accumulate there. To further use the results and compare them to surface tension data, actual surface concentrations are estimated from the resulting XPS intensities. For this purpose, different approaches are introduced and the resulting surface concentration estimates are used to model surface tension. The comparison to experimentally determined surface tension data served as validation of the approaches. With the presented results in papers I to III on the surface composition of pure solutions containing only one solute and the successful comparison to macroscopic properties, one can approach more complicated aqueous systems containing two or more solutes, with the aim to disentangle their respective contributions to net properties of the solution.

In the second part, results of mixed solutions containing different ions or molecules in an electrolyte solution are discussed. The comparison of guanidinium and ammonium ions, which are important functional groups of common amino acids, is yet another demonstration that ions can reside close to the

aqueous surface, despite of what is expected from the classic picture [95, 96]. Nevertheless, not the ion's size is the decisive parameters here, as it is proposed for big halide ions, but the asymmetric solvation shell. Guanidinium forms strong hydrogen bonds with water within the plane, while the flat faces do not interact with water significantly. Hence, in parallel orientation, guanidinium can approach closely to the aqueous surface. Furthermore, the study also reveals that guanidinium is pushed even closer to the surface in the presence of ammonium ions in solution. According to the well-known salting-out effect, succinic acid is enhanced at the air-water interface when co-dissolved with inorganic ions. This increases the surface concentration of the neutral species, which was quantified using a Langmuir-adsorption-based model with extension for added inorganic salts. The implications of the presented results on atmospheric aerosol particles and their properties are discussed, where a strong correlation between size and organic acid loading is established. This finding enables to draw conclusions on the phase state of atmospheric nanoparticles.

Looking back on the results that were obtained throughout the last years, it is clear that results from surface-sensitive XPS experiments give further insights into the structure of aqueous solutions. Especially its chemical sensitivity should be emphasized in this context, since many other methods used to study the surface of aqueous solutions lack that property. With new spectrometers that allow to conduct experiments at even higher background pressures and with the higher photon intensities of new synchrotron facilities, further and more detailed studies will be possible.

Using a liquid micro-jet, a major limitation is the solubility of a compound. It is obviously not possible to study supersaturated solutions or even partially crystallized samples. Therefore, the further development of an aerosol injector, which transports aerosol particles into the interactions zone of the spectrometer, is an essential next step in order to be able to show the connection between dilute aqueous solutions and aerosol particles containing different amounts of water.

Another aspect of great importance is dynamics in liquids. The development of pump-probe laser setups that allow for time-resolved probing of core-levels will open new possibilities enabling e.g. the direct monitoring of cooling or warming of aqueous solutions. In combination with XPS, this allows for example the study of the spatial distribution of solutes at the aqueous surface as a function of temperature with surface sensitivity and chemical specificity.

7. Summary in Swedish: Att utforska ytan hos vattenlösningar

Vatten och vattenlösningar finns överallt på jorden i många olika former: hav, sjöar, regn, moln och i levande organismer. Vatten har mycket speciella egenskaper. Till exempel expanderar vatten när det fryser och har maximal densitet vid 4 °C. Vattenmolekylen är uppbyggd av två väteatomer och en syreatom. Syreatomen drar delvis till sig elektroner från de båda vätena vilket gör att syre- och väteatomerna från olika vattenmolekyler attraherar varandra i så kallade vätebindningar. De fysikaliska och kemiska egenskaperna hos vatten bestäms i hög grad av dessa vätebindningar som är organiserade i tredimensionella nätverk. Det är vattnets förmåga att bilda vätebindningar och de polära egenskaperna som gör att många föreningar, främst de som är laddade, löses lätt och därmed kan de transporteras med vattnet. Ämnen som löser sig bra i vatten kallar man för hydrofila, medan ämnen som inte är lösliga i vatten kallas för hydrofoba. Vatten omsätts i naturen i ett eget kretslopp där vatten förflyttas mellan hav, sjöar, vattendrag, atmosfären, yt- och grundvatten, samt levande organismer. De viktigaste processerna för detta kretslopp är avdunstning, kondensation och nederbörd.

Denna doktorsavhandling handlar främst om ytskiktet hos vattenlösningar, då detta spelar en stor roll speciellt i små droppar, något som det finns mycket av i atmosfären. På grund av dessa droppars storlek är deras förhållande mellan yta och volym mycket stort. Förändringar vid gränsskiktet är speciellt viktiga eftersom de kan förändra egenskaperna hos mycket små atmosfäriska droppar på ett betydande sätt. Förutom de makroskopiska egenskaperna, som till exempel reflektion av solljus och ytspänning, studerar många forskargrupper också yteffekter på mikroskopisk nivå [1, 2]. Man vill lära sig mer om reaktioner mellan luft och ytskiktet hos vattendroppar. En frågeställning är hur lätt det är för en vattendroppe att ta upp ett visst ämne från luften samt att kvantifiera hur mycket som tas upp [46, 114]. En annan viktig aspekt handlar om ytans struktur och sammansättning. Sammansättningen av ytregionen spelar en avgörande roll för vattendroppens egenskaper, eftersom detta skikt är i direkt kontakt med den omgivande luften. Genom att bestämma sammansättningen och därmed även fördelningen av ämnen i ytan, blir det möjligt att uppskatta vattendroppens kemiska och fysikaliska egenskaper.

I denna avhandling presenteras fem artiklar som beskriver experimentella studier där fördelningen av olika kemiska ämnen vid ytan hos vattenlösningar har undersökts. Den huvudsakliga experimentella metoden som använts är röntgeninducerad fotoelektronspektroskopi, som oftast förkortas till XPS (X-ray Photoelectron Spectroscopy) eller ESCA (Elektron-Spectroscopy for

Chemical Analysis). XPS- eller ESCA-metoden utvecklades vid Uppsala universitet av K. Siegbahn och hans medarbetare [55]. K. Siegbahn delade Nobelpriset i fysik för utvecklingen av denna teknik 1981.

I ett XPS-experimentet skjuter man fotoner med en viss energi på atomerna i ett material. Om fotonenergin är tillräcklig hög, kan man slå ut elektroner från materialet. De utsända elektronerna blir därefter infångade och deras kinetiska energi blir bestämd. Intensiteten av elektronerna avsätts sedan i en graf som funktion av elektronernas bindningsenergi, vilket är skillnaden mellan fotonenergin och kinetiska energin hos de utsända elektronerna. Denna graf kallas för ett fotoemissionsspektrum. Bindningsenergierna är unika för varje ämne i periodiska systemet, vilket tillåter XPS-metoden att bestämma vilka grundämnen det finns i ett material. Dessutom förskjuts bindningsenergin lite beroende på vilka grannatomer en atom har i ett material. Detta gör det möjligt att till exempel skilja mellan den protonerade eller oprotonerade formen av en syra i lösning. Förutom den kemiska känsligheten, så kan man undersöka ytans djupprofil på ett unikt sätt med XPS. Fotonerna som träffar provet tränger olika djupt in i provet beroende på dess energi och längs med dess väg slås elektroner ut. De elektroner som sänts ut från en atom djupt inne i materialet studsar inelastiskt, dvs. med energiförlust, med andra atomer i det täta materialet. Därför kan man i princip inte detektera elektroner från atomer djupare än de i de yttersta atom- eller molekyllagren. Elektroner som sänds ut av en atom i ytskiktet kan å andra sidan snabbt lämna det täta materialet och detekteras i spektrometern, vilket är förklaringen till att XPS-metoden är ytkänslig.

Det är en experimentell utmaning att använda XPS på vattenlösningar, eftersom experiment måste utföras i vakuum på grund av den korta vägen elektroner kan röra sig genom luft utan att absorberas. Flyktiga vätskeprover är en speciell utmaning, då de höjer trycket i den experimentella uppställningen genom att dunsta av. Tekniska utvecklingar främst utförda av M. Faubel och medarbetare [10], möjliggör användningen av XPS på vattenprover genom att introducera lösningen som en tunn stråle in i en vakuumkammare. Eftersom man behöver fotoner med olika energier utför man oftast XPS-experiment vid synkrotronljusanläggningar. Dessa anläggningar levererar röntgenstrålning med hög intensitet i ett brett spektrum av våglängder. Alla experiment som är presenterade i denna doktorsavhandling är utförda vid den svenska synkrotronljusanläggningen MAX-lab i Lund.

I denna avhandling har XPS tillämpats på vattenlösningar med olika upplösta ämnen för att samla information om mikroskopiska sammansättningen av ytskiktet. De presenterade studierna är främst motiverade av miljö- och atmosfärsvetenskap. De valda systemen representerar typiska modellsystem, som liknar verkliga lösningar som finns i naturen, till exempel i molndroppar eller biologiska celler. Föreningar, som tros spela en framträdande roll i aerosolers aktiverings- och tillväxtprocesser [11], såsom lågflyktiga organiska föreningar, studerades. Joner anses i allmänhet vara utarmade i

vattenytan. Tidigare studier har visat att stora halid- och oxoanjoner med låg laddning, som t. ex. jodid- och perkloratjonerna, har visat en benägenhet att uppehålla sig i närheten av ytan [3, 4]. Dessa egenskaper är inte väl studerade för många andra salter och framförallt blandningar av salter, som liknar mer verkliga lösningar.

I den första delen av avhandlingen beskrivs resultat av vattenlösningar som innehåller bärnstenssyra ($HOOC(CH_2)_2COOH$) eller olika alkylalkoholer ($C_nH_{2n+1}OH$). Dessa molekyler består av både en hydrofil och en hydrofob del, vilka också kallas amfifiler. Koncentrationsberoende XPS-mätningar av bärnstenssyra och olika alkylalkoholer i vattenlösningar, har analyserats med hjälp av olika metoder som tillåter kvantifiering av ytkoncentrationer, där även parametrar såsom surhetsgrad (pH) och förgreningen av alkylkedjan varierades. Det visade sig att ytkoncentrationen är mycket högre än deras bulkkoncentration för de studerade molekylerna. På grund av metodens känslighet till kemiska tillstånd, kunde även orienteringen av linjära och grenade alkylalkoholer som en funktion av koncentrationen undersökas. Alkoholmolekyler med långa raka alkylkedjor "ställer sig upp" vid höga bulkkoncentrationer för att kunna forma ett tätt skikt på ytan. Denna omorientering har sitt ursprung i de hydrofila och hydrofoba interaktionerna mellan molekylerna och vattnet i gränsregionen. Strax under gränsskiktet mellan luft och vatten slutar det tredimensionella vätebindningsnätverket av vattnet och de nämnda interaktionerna kan driva molekylerna till en viss ordning.

I den andra delen av avhandlingen behandlas lösningar som innehåller mer än en förening. I en av studierna undersöktes blandade lösningar som är viktiga inom biokemi, bland annat guanidinium- och ammoniumjonerna, $[C(NH_2)_3]^+$ respective NH_4^+. Dessa joner är viktiga funktionella grupper i till exempel aminosyror. Verkliga biokemiska system såsom proteiner eller DNA är oftast ganska svåra att undersöka direkt. Studier av viktiga funktionella grupper ger således värdefull information som möjliggör förståelsen av framtida resultat på mer komplexa system. Återigen varierades koncentrationen, men även lösningar innehållande elektrolyter studerades där skillnader i den rumsliga fördelningen och ytregionens sammansättning var av särskilt intresse. Resultaten visar att den platta guanidiniumjonen har en tydlig benägenhet att uppehålla sig vid ytan, vilket förklaras av stark hydratation i endast två dimensioner. De unika hydratationsskalen tillåter guanidiniumjoner att komma nära vattenytan, om jonen är orienterad parallellt med ytan. Dessutom visades att guanidiniumjoner trycks ännu närmare ytan av ammoniumjoner i lösningar med båda jonerna närvarande. I den andra studien, där bärnstenssyra i elektrolytlösningar med olika koncentration och sammansättning studerades, visades att närvaron av elektrolyter ökade syrans förekomst i gränsregionen. Vidare kvantifierades effekterna genom att uppskatta ytkoncentrationen som en funktion av bulkkoncentrationen. Sammanfattningsvis diskuteras hur de erhållna resultaten påverkar bilden av atmosfäriska vattendroppars kemiska och fysikaliska uppträdande.

List of abbreviations

BE	binding energy
C_C	carbon atom in alkyl-chain
C_{OH}	carbon atom, where the hydroxyl group is attached to
C_{COO^-}	carbon atom in deprotonated carboxylic acid group
C_{COOH}	carbon atom in carboxylic acid group
CCN	cloud condensation nuclei
DNA	deoxyribonucleic acid
E_{kin}	kinetic energy of a photoelectron
EAL	effective attenuation length
ESCA	electron spectroscopy for chemical analysis
FWHM	full width at half maximum
Gdm^+	guanidinium ion, $[C(NH_2)_3]^+$
GdmCl	guanidinium chloride, $C(NH_2)_3Cl$
m	molal concentration in [mol/kg H_2O]
M	molar concentration in [mol/dm^3]
MD	molecular dynamics
NMR	nuclear magnetic resonance
PCI	post collision interaction
PE	photoemission
RH	relative humidity
$SuccH_2$	succinic acid
$Succ^{2-}$	divalent succinate ion
x	mole fraction
XPS	X-ray photoelectron spectroscopy
ΔG^{ads}	Gibbs free energy of adsorption

Acknowledgments

I had the pleasure to get to know so many inspiring and brilliant people during these last four and a half years. This text cannot in any ways live up to how grateful I am to got to know you and I hope, if I haven't done so, I get a chance to tell you in person one day.

I would like to express my gratitude to both universities, Uppsala University and the Swedish University of Agricultural Sciences, for accepting me for graduate studies and letting me be part of two great departments. This project was initiated by my two main supervisors: Olle Björneholm and Ingmar Persson, who decided to hire me as a PhD student. You are an unbeatable team - probably because you are both so different characters, and in combination the best that could happen to me!

Olle has the great gift to always be there for the *big* decisions and when new ideas needed to be established. Thanks for always supporting me and giving me the freedom to take my own steps. It was great that you let me be part of inspiring scientific discussions and new collaborations, whenever possible.

Ingmar took me often to a journey, back to basic chemistry - which was more than necessary at times! Thanks for discussing all my questions with endless patience. You are a great teacher and I'll always try to have your encouragements and experienced advice in mind.

Johan and Daniel, my two assistant supervisors, who helped me getting started back in 2011 and were always up for discussions about all kinds of things. Thanks for being there for me, whenever I needed advice.

I greatly thank the *extended* liquid-jet-team for all the exciting experiments, happy and frustrating times at the synchrotron, and endless discussions of our results. The core of the group for a long time consisted of Gunnar, Victor, Madeleine, Win Win and lately also Clara, as well as Arnaldo and Ricardo from Brazil. Thanks especially to Gunnar, who knows everything about X-ray sciences and every detail of a Scienta spectrometer. You saved us many times and knew how to fix a problem - even on the phone. Victor and I spent probably most beamtimes together, which was always great fun. I hope the new MAX-lab has no surprise showers for you - tummenar upp! I'd also like to thank Madeleine for all the great discussions. I admire you for the structured and skilled way of going upon a project.

All the experiments at MAX-lab would have not been possible without the help of the staff: Maxim, Mikko, Marcin, Carro and everyone else around - you made those many weeks of beamtime more pleasant and helped whenever possible, especially when the experiment turned itself against us.

I take this opportunity to thank all my colleges in the division of molecular and condensed matter physics at Ångström. Håkan and Charlie, your enthusiasm and lively nature is contagious and you gave me the feeling of being a relevant part of this division. Rein always has the right O-rings or tools at hand and helped me a lot together with the incredible team of the mechanics workshop to repair or design new experimental equipment. Olof, Victor and Johan O., it was great to prepare and teach course labs with you. Thanks also to everyone for the joyful discussions during the fika-breaks and lunches: Ruben, Anders, Maria, Sergei, Dimitri, Laurent, Ute, Ronny, Torsten, Sareh, Svante, Yasmine, Carla, Robert, Joachim, Valeria, Roberta, Christrofer, Nial, Fredrik, Richard, Mattias, Nils M., Stefan, Somnath, Dibyah, Teng, Corina, Yevgen, Nic, Calle, Marcus, Felix, Bertrand, Rebecka, Susanna, Andreas S., Andreas L., Magnus, Minjie, Nils K., Hans, Joseph and many more. Nina and Melanie, it was great to share the office with you for a while! Special thanks goes also to Davide: you are a gifted teacher and with your dedication to IGOR Pro, you made me learn how to write awesome procedures. Delphine - so great that you joined our group, I loved working with you! Ieva, the time we were together here in Uppsala was awesome. We were always planning to do so many things and often thought we wouldn't make any oft it - but in fact, we made sooo many things happen too!

I would also like to thank my colleges at SLU for your support, even if I couldn't be present as frequently as I would have wished: Anke, Tobias, Gunnar, Elisabeth, Ning, Johan and Shahin - it was always nice to have you around. Yina and Önder, it was great to discuss our project together.

Greetings to my PhD fellows at other places: Anna and Ågot in Gothenburg, Elin in Lund, Sara in Stockholm and Isaak and Stephan in Berlin, you are the greatest company for conferences, summer schools, beamtimes and also free time! Thanks goes also to Li, Sebastian, Carla, Joachim and Peli for the after works and lunches every now and then.

I want to acknowledge my collaborators for the discussion of our project, their patience and help. I'd like to especially thank Erik and Pavel, who helped me writing my first first-author publication - you were incredibly patient and encouraged me along the way. Ilona, Maryam and Jan, who I was lucky enough to work on two publications together - thanks for this great experience, I learned a lot from you. Greetings go also to Joakim, Axel and Ville - it's so great that we managed to combine our setups and measured on soot particles!

Finally I'd like to thank my family and friends, both near and far, for all your encouragement, support and for listening to me, in cheerful and frustrated times. Without your support I would have never made it! Fredrik, there are no words to describe your part in this journey: thank you for everything!

References

[1] P. Jungwirth and D. J. Tobias, *Chem. Rev.*, 2006, **106**, 1259–1281.

[2] P. B. Petersen and R. J. Saykally, *Annu. Rev. Phys. Chem.*, 2006, **57**, 333–364.

[3] N. Ottosson, R. Vácha, E. F. Aziz, W. Pokapanich, W. Eberhardt, S. Svensson, G. Öhrwall, P. Jungwirth, O. Björneholm and B. Winter, *J. Chem. Phys.*, 2009, **131**, 1247061–1247067.

[4] L. Piatkowski, Z. Zhang, E. H. G. Backus, H. J. Bakker and M. Bonn, *Nat. Commun.*, 2014, **5**, 4083–4089.

[5] P. B. Petersen and R. J. Saykally, *Chem. Phys. Lett.*, 2008, **458**, 255–261.

[6] H. Mishra, S. Enami, R. J. Nielsen, L. A. Stewart, M. R. Hoffmann, W. A. Goddard and A. J. Colussi, *Proc. Natl. Acad. Sci. USA*, 2012, **109**, 18679–18683.

[7] R. J. Saykally, *Nat. Chem.*, 2013, **5**, 82–84.

[8] Intergovernmental Panel on Climate Change, *Climate Change 2013: The physical science basis: Working group I contribution to the fifth assessment report of the Intergovernmental Panel on Climate Change*, Cambridge University Press, 2014.

[9] H. Siegbahn and K. Siegbahn, *J. Electron. Spectrosc. Relat. Phenom.*, 1973, **2**, 319 – 325.

[10] M. Faubel, S. Schlemmer and J. P. Toennies, *Z. Phys. D Atoms, Mol. Clust.*, 1988, **10**, 269–277.

[11] M. Ehn, J. A. Thornton, E. Kleist, M. Sipilä, H. Junninen, I. Pullinen, M. Springer, F. Rubach, R. Tillmann, B. Lee, F. Lopez-Hilfiker, S. Andres, I.-H. Acir, M. Rissanen, T. Jokinen, S. Schobesberger, J. Kangasluoma, J. Kontkanen, T. Nieminen, T. Kurten, L. B. Nielsen, S. Jørgensen, H. G. Kjaergaard, M. Canagaratna, M. D. Maso, T. Berndt, T. Petäjä, A. Wahner, V.-M. Kerminen, M. Kulmala, D. R. Worsnop, J. Wildt and T. F. Mentel, *Nature*, 2014, **506**, 476–479.

[12] M. A. Henderson, *Surf. Sci. Rep.*, 2002, **46**, 1–308.

[13] K. Kimura, S. Katsumata, Y. Achiba, T. Yamazaki and S. Iwata, *Handbook of He I Photoelectron Spectra of Fundamental Organic Molecules. Ionization Energies, Ab Initio Assignments, and Valence Electronic Structure for 200 Molecules*, Japan Scientific Societies Press and Halstead Press, Tokyo, 1981.

[14] B. Winter, R. Weber, W. Widdra, M. Dittmar, M. Faubel and I. Hertel, *J. Phys. Chem. A*, 2004, **108**, 2625–2632.

[15] K. A. Sharp and J. M. Vanderkooi, *Acc. Chem. Res.*, 2010, **43**, 231–239.

[16] D. R. Lide, *CRC handbook of chemistry and physics*, CRC press, 2004.

[17] D. W. Smith, *J. Chem. Educ.*, 1977, **54**, 540–542.

[18] A. A. Zavitsas, *J. Phys. Chem. B*, 2001, **105**, 7805–7817.

[19] M. Tuckerman, K. Laasonen, M. Sprik and M. Parrinello, *J. Phys. Chem.*, 1995, **99**, 5749–5752.

[20] C. D. Cappa, J. D. Smith, B. M. Messer, R. C. Cohen and R. J. Saykally, *J. Phys. Chem. A*, 2007, **111**, 4776–4785.

[21] E. F. Aziz, N. Ottosson, M. Faubel, I. V. Hertel and B. Winter, *Nature*, 2008, **455**, 89–91.

[22] J. S. Hub, M. G. Wolf, C. Caleman, P. J. van Maaren, G. Groenhof and D. van der Spoel, *Chem. Sci.*, 2014, **5**, 1745–1749.

[23] P. Atkins and J. de Paula, *Atkins' Physical Chemistry*, OUP Oxford, 2010.

[24] M. Silberberg, *Chemistry: the molecular nature of matter and change*, McGraw-Hill, 2002.

[25] A. Holleman, E. Wiberg and N. Wiberg, *Lehrbuch der anorganischen Chemie*, de Gruyter, 1995.

[26] P. L. Silvestrelli and M. Parrinello, *Phys. Rev. Lett.*, 1999, **82**, 3308–3311.

[27] D. Spångberg and K. Hermansson, *J. Chem. Phys.*, 2004, **120**, 4829–4843.

[28] S. Rajamani, T. Ghosh and S. Garde, *J. Chem. Phys.*, 2004, **120**, 4457–4466.

[29] R. G. Weiß, M. Heyden and J. Dzubiella, *Phys. Rev. Lett.*, 2015, **114**, 1878021–1878025.

[30] G. N. Lewis, *J. Am. Chem. Soc.*, 1908, **30**, 668–683.

[31] A. Fredenslund, R. L. Jones and J. M. Prausnitz, *AIChE J.*, 1975, **21**, 1086–1099.

[32] J. Gmehling, R. Wittig, J. Lohmann and R. Joh, *Ind. Eng. Chem. Res.*, 2002, **41**, 1678–1688.

[33] S. L. Clegg and J. H. Seinfeld, *J. Phys. Chem. A*, 2006, **110**, 5692–5717.

[34] Y. Marcus and G. Hefter, *Chem. Rev.*, 2006, **106**, 4585–4621.

[35] R. Buchner, S. G. Capewell, G. Hefter and P. M. May, *J. Phys. Chem. B*, 1999, **103**, 1185–1192.

[36] M. V. Fedotova and S. E. Kruchinin, *J. Mol. Liq.*, 2011, **164**, 201–206.

[37] H. N. Po and N. M. Senozan, *J. Chem. Educ.*, 2001, **78**, 1499–1503.

[38] M. J. Rosen and J. T. Kunjappu, *Surfactants and interfacial phenomena*, Wiley, 2012.

[39] F. B. Sprow and J. M. Prausnitz, *Trans. Faraday Soc.*, 1966, **62**, 1097–1104.

[40] F. B. Sprow and J. M. Prausnitz, *Trans. Faraday Soc.*, 1966, **62**, 1105–1111.

[41] Z.-B. Li, Y.-G. Li and J.-F. Lu, *Ind. Eng. Chem. Res.*, 1999, **38**, 1133–1139.

[42] E. McCash, *Surface Chemistry*, Oxford University Press, 2001.

[43] J. Seinfeld and S. Pandis, *Atmospheric chemistry and physics: from air pollution to climate change*, Wiley, 1998.

[44] H. Köhler, *Trans. Faraday Soc.*, 1936, **32**, 1152–1161.

[45] M. D. Petters and S. M. Kreidenweis, *Atmos. Chem. Phys.*, 2007, **7**, 1961–1971.

[46] D. K. Farmer, C. D. Cappa and S. M. Kreidenweis, *Chem. Rev.*, 2015, **115**, 4199–4217.

[47] J.-P. Chen, *J. Atmos. Sci.*, 1994, **51**, 3505–3516.

[48] M. L. Shulman, M. C. Jacobson, R. J. Carlson, R. E. Synovec and T. E. Young, *Geophys. Res. Lett.*, 1996, **23**, 277–280.

[49] M. C. Facchini, M. Mircea, S. Fuzzi and R. J. Charlson, *Nature*, 1999, **401**, 257–259.

[50] R. Sorjamaa, B. Svenningsson, T. Raatikainen, S. Henning, M. Bilde and A. Laaksonen, *Atmos. Chem. Phys.*, 2004, **4**, 2107–2117.

[51] Y. Cheng, H. Su, T. Koop, E. Mikhailov and U. Pöschl, *Nat. Commun.*, 2015, **6**, 5923–5929.

[52] S. Hüfner, *Photoelectron Spectroscopy: Principles and Applications*, Springer-Verlag Berlin Heidelberg, 1995.

[53] J. Stöhr, *NEXAFS Spectroscopy*, Springer, 1992.

[54] A. Einstein, *Ann. Phys.*, 1905, **322**, 132–148.

[55] K. Siegbahn, C. Nordling and A. Fahlman, *Nov. Act. Uppsaliensis*, 1967.

[56] A. Thompson, D. Attwood, E. Gullikson, M. Howells, K.-J. Kim, J. Kirz, J. Kortright, I. Lindau, P. Pianetta, A. Robinson, J. Scofield, J. Underwood, D. Vaughan, G. Williams and H. Winick, *X-Ray Data Booklet*, Lawrence Berkeley Laboratory, 2001.

[57] T. Koopmans, *Physica*, 1934, **1**, 104 – 113.

[58] W. Heisenberg, *Z. Phys.*, 1927, **43**, 172–198.

[59] J. L. Campbell and T. Papp, *At. Data Nucl. Data Tables*, 2001, **77**, 1 – 56.

[60] A. Jablonski and C. Powell, *J. Electron. Spectrosc. Relat. Phenom.*, 1999, **100**, 137–160.

[61] N. Ottosson, M. Faubel, S. E. Bradforth, P. Jungwirth and B. Winter, *J. Electron. Spectrosc. Relat. Phenom.*, 2010, **177**, 60–70.

[62] H. Nikjoo, S. Uehara, D. Emfietzoglou and A. Brahme, *New J. Phys.*, 2008, **10**, 1–28.

[63] S. Thürmer, R. Seidel, M. Faubel, W. Eberhardt, J. C. Hemminger, S. E. Bradforth and B. Winter, *Phys. Rev. Lett.*, 2013, **111**, 1730051–1730055.

[64] O. Björneholm, J. Werner, N. Ottosson, G. Öhrwall, V. Ekholm, B. Winter, I. Unger and J. Söderström, *J. Phys. Chem. C*, 2014, **118**, 29333–29339.

[65] J. Cooper and R. N. Zare, *J. Chem. Phys.*, 1968, **48**, 942–943.

[66] J. A. R. Samson, *J. Opt. Soc. Am.*, 1969, **59**, 356–357.

[67] R. F. Reilman, A. Msezane and S. T. Manson, *J. Electron. Spectrosc. Relat. Phenom.*, 1976, **8**, 389–394.

[68] J. Söderström, N. Mårtensson, O. Travnikova, M. Patanen, C. Miron, L. J. Sæthre, K. J. Børve, J. J. Rehr, J. J. Kas, F. D. Vila, T. D. Thomas and S. Svensson, *Phys. Rev. Lett.*, 2012, **108**, 1930051–1930054.

[69] T. X. Carroll, M. G. Zahl, K. J. Børve, L. J. Sæthre, P. Decleva, A. Ponzi, J. J. Kas, F. D. Vila, J. J. Rehr and T. D. Thomas, *J. Chem. Phys.*, 2013, **138**, 234310 – 234315.

[70] H. Siegbahn, *J. Phys. Chem.*, 1985, **89**, 897–909.

[71] M. Bässler, J.-O. Forsell, O. Björneholm, R. Feifel, M. Jurvansuu, S. Aksela, S. Sundin, S. Sorensen, R. Nyholm, A. Ausmees and S. Svensson, *J. Electron. Spectrosc. Relat. Phenom.*, 1999, **101 - 103**, 953–957.

[72] M. Bässler, A. Ausmees, M. Jurvansuu, R. Feifel, J.-O. Forsell, P. de Tarso Fonseca, A. Kivimäki, S. Sundin, S. Sorensen, R. Nyholm, O. Björneholm, S. Aksela and S. Svensson, *Nucl. Instr. Meth. Phys. Res. A*, 2001, **469**, 382–393.

[73] M. A. Brown, M. Faubel and B. Winter, *Annu. Rep. Prog. Chem., Sect. C*, 2009, **105**, 174–212.

[74] D. E. Starr, E. K. Wong, D. R. Worsnop, K. R. Wilson and H. Bluhm, *Phys. Chem. Chem. Phys.*, 2008, **10**, 3093–3098.

[75] M. A. Brown, A. B. Redondo, I. Jordan, N. Duyckaerts, M.-T. Lee, M. Ammann, F. Nolting, A. Kleibert, T. Huthwelker, J.-P. Müächler, M. Birrer, J. Honegger, R. Wetter, H. J. Wörner and J. A. van Bokhoven, *Rev. Sci. Instrum.*, 2013, **84**, 0739041–0739048.

[76] B. Winter and M. Faubel, *Chem. Rev.*, 2006, **106**, 1176–1211.

[77] J. R. Jones, D. L. G. Rowlands and C. B. Monk, *Trans. Faraday Soc.*, 1965, **61**, 1384–1388.

[78] D. E. Bidstrup and C. J. Geankoplis, *J. Chem. Eng. Data*, 1963, **8**, 3–6.

[79] G. Öhrwall, N. L. Prisle, N. Ottosson, J. Werner, V. Ekholm, M.-M. Walz and O. Björneholm, *J. Phys. Chem. B*, 2015, **119**, 4033–4040.

[80] P. van der Straten, R. Morgenstern and A. Niehaus, *Z. Phys. D*, 1988, **8**, 35–45.

[81] J. Yeh and I. Lindau, *At. Data Nucl. Data Tables*, 1985, **32**, 1 – 155.

[82] N. L. Prisle, N. Ottosson, G. Öhrwall, J. Söderström, M. Dal Maso and O. Björneholm, *Atmos. Chem. Phys.*, 2012, **12**, 12227–12242.

[83] R. M. Onorato, D. E. Otten and R. J. Saykally, *Proc. Natl. Acad. Sci. USA*, 2009, **106**, 15176–15180.

[84] K. A. Perrine, M. H. C. Van Spyk, A. M. Margarella, B. Winter, M. Faubel, H. Bluhm and J. C. Hemminger, *J. Phys. Chem. C*, 2014, **118**, 29378–29388.

[85] P. Jungwirth and B. Winter, *Annu. Rev. Phys. Chem.*, 2008, **59**, 343–366.

[86] R. Seidel, S. Thürmer and B. Winter, *J. Phys. Chem. Lett.*, 2011, **2**, 633–641.

[87] H. Singh, Y. Chen, A. Staudt, D. Jacob, D. Blake, B. Heikes and J. Snow, *Nature*, 2001, **410**, 1078–1081.

[88] M. Hallquist, J. C. Wenger, U. Baltensperger, Y. Rudich, D. Simpson, M. Claeys and J. Dommen, *Atmos. Chem. Phys.*, 2009, **9**, 5155–5236.

[89] N. L. Prisle, T. Raatikainen, R. Sorjamaa, B. Svenningsson, A. Laaksonen and M. Bilde, *Tellus B*, 2011, **60**, 416–431.

[90] J. Vanhanen, A.-P. Hyvärinen, T. Anttila, T. Raatikainen, Y. Viisanen and H. Lihavainen, *Atmos. Chem. Phys.*, 2008, **8**, 4595–4604.

[91] A. A. Zardini, I. Riipinen, I. K. Koponen, M. Kulmala and M. Bilde, *J. Aerosol Sci.*, 2010, **41**, 760–770.

[92] T. Yli-Juuti, A. A. Zardini, A. C. Eriksson, A. M. K. Hansen, J. H. Pagels, E. Swietlicki, B. Svenningsson, M. Glasius, D. R. Worsnop, I. Riipinen and M. Bilde, *Environ. Sci. Technol.*, 2013, **47**, 12123–12130.

[93] J. Gliński, G. Chavepeyer, J.-K. Platten and P. Smet, *J. Chem. Phys.*, 1998, **109**, 5050–5053.

[94] S. Can, D. Mago, O. Esenturk and R. Walker, *J. Phys. Chem. C*, 2007, **111**, 8739–8748.

[95] L. Onsager and N. N. T. Samaras, *J. Chem. Phys.*, 1934, **2**, 528–536.

[96] D. H. Andrews, *J. Chem. Educ.*, 1929, **6**, 591–592.

[97] R. Taft and F. Welch, *Trans. Kans. Acad. Sci.*, 1951, **54**, 233–246.

[98] S. A. Lowry, M. H. Mccay, T. D. McCay and P. A. Gray, *J. Cryst. Growth*, 2000, **96**, 774–776.

[99] J. D. Roberts, *Acc. Chem. Res.*, 2006, **39**, 889–896.

[100] P. G. Blower, S. T. Ota, N. A. Valley, S. R. Wood and G. L. Richmond, *J. Phys. Chem. A*, 2013, **117**, 7887–7903.

[101] C. R. Ruehl and K. R. Wilson, *J. Phys. Chem. A*, 2014, **118**, 3952–3966.

[102] T. Raatikainen and A. Laaksonen, *Atmos. Chem. Phys.*, 2005, **5**, 2475–2495.

[103] S. Garde, *Nature*, 2015, **517**, 277–279.

[104] D. J. Donaldson and V. Vaida, *Chem. Rev.*, 2006, **106**, 1445–1461.

[105] A. Zuend and J. H. Seinfeld, *Atmos. Chem. Phys.*, 2012, **12**, 3857–3882.

[106] N. Ottosson, J. Heyda, E. Wernersson, W. Pokapanich, S. Svensson, B. Winter, G. Öhrwall, P. Jungwirth and O. Björneholm, *Phys. Chem. Chem. Phys.*, 2010, **12**, 10693–10700.

[107] Y. Marcus, *J. Chem. Thermodyn.*, 2012, **48**, 70–74.

[108] D. R. Rosseinsky, *Chem. Rev.*, 1965, **65**, 467–490.

[109] P. E. Mason, G. W. Nielson, J. E. Enderby, M.-L. Saboungi, C. E. Dempsey, J. A. D. MacKerell and J. W. Brady, *J. Am. Chem. Soc.*, 2004, **126**, 11462–11470.

[110] D. Bandyopadhyay, K. Bhanja, S. Mohan, S. K. Ghosh and N. Choudhury, *J. Phys. Chem. B*, 2015, **119**, 11262–11274.

[111] M. Vazdar, J. Vymětal, J. Heyda, J. Vondrášek and P. Jungwirth, *J. Phys. Chem. A*, 2011, **115**, 11193–11201.

[112] O. Shih, A. H. England, G. C. Dallinger, J. W. Smith, K. C. Duffey, R. C. Cohen, D. Prendergast and R. J. Saykally, *J. Chem. Phys.*, 2013, **139**, 0351041–03510417.

[113] E. Wernersson, J. Heyda, M. Vazdar, M. Lund, P. E. Mason and P. Jungwirth, *J. Phys. Chem. B*, 2011, **115**, 12521–12526.

[114] M. Kanakidou, J. H. Seinfeld, S. N. Pandis, I. Barnes, F. J. Dentener, M. C. Facchini, R. Van Dingenen, B. Ervens, A. Nenes, C. J. Nielsen, E. Swietlicki, J. P. Putaud, Y. Balkanski, S. Fuzzi, J. Horth, G. K. Moortgat, R. Winterhalter, C. E. L. Myhre, K. Tsigaridis, E. Vignati, E. G. Stephanou and J. Wilson, *Atmos. Chem. Phys.*, 2005, **5**, 1053–1123.

[115] D. P. Veghte, M. B. Altaf and M. A. Freedman, *J. Am. Chem. Soc.*, 2013, **135**, 16046–16049.

[116] O. Laskina, H. S. Morris, J. R. Grandquist, Z. Qin, E. A. Stone, A. V. Tivanski and V. H. Grassian, *J. Phys. Chem. A*, 2015, **119**, 4489–4497.

[117] A. M. Booth, D. O. Topping, G. Mcfiggans and C. J. Percival, *Phys. Chem. Chem. Phys.*, 2009, **11**, 8021–8028.

[118] L. T. Padró, A. Asa-Awuku, R. Morrison and A. Nenes, *Atmos. Chem. Phys.*, 2007, **7**, 5263–5274.

[119] M. Bilde and B. Svenningsson, *Tellus B*, 2004, **56**, 128–134.

[120] S. Henning, T. Rosenørn, B. D'Anna, A. A. Gola, B. Svenningsson and M. Bilde, *Atmos. Chem. Phys.*, 2005, **5**, 575–582.